Petrogenesis and PGE of the lower mineralized zone of the Waterberg Project, South Africa

August 28, 2017

Huthmann, Yudovskaya, Kinnaird, McCreesh, McDonald

Abstract

The Waterberg deposit is located north of the Northern Lobe of the Bushveld Complex in South Africa and represents a large, high-grade, new PGE discovery with the potential to change the local and global ~~mining~~PGE market. The first comprehensive study of the lower ultramafic section of ~~this~~the ~~exciting~~ area has been ~~conducted~~completed, and ~~below~~ ~~core logging,~~ whole-rock chemical analysi~~s~~es and ~~six element~~ PGE data are presented.

The ~~Waterberg Succession in the s~~section studied comprises mineralized harzburgite~~s~~ and marginal orthopyroxenite, ~~rocks~~ overlain by troctolite grading into gabbroic rocks.~~–~~ Whole-rock analyses show geochemical ~~signatures~~variations typical of differentiated assemblages of cumulus olivine, plagioclase, and pyroxene ~~assemblages~~. Normalized trace element data display HREE depletion, strong positive Eu and Sr anomalies and LREE enrichment. The ~~position of positive as well as negative~~negative anomalies for Th, Rb, Nb and Ta ~~is~~are typical for rocks of the Bushveld Complex. Normalized PGE distributions are ~~strongly~~ fractionated (Pd/Ir 177) ~~and~~, Pd-enriched, and Au-poor.~~.~~

Emplacement of the ~~rocks~~magmas ~~was initiated~~is believed to have commenced ~~by~~with west-east trending, finger-like intrusions, followed by lateral dilation and emplacement of sulfide droplet-bearing, ultramafic ~~chonoliths~~magmas. This ~~in turn~~ was followed by a second phase of intrusi~~ve~~ons, characterized by sheet-like ~~emplacement~~bodies of troctolites. Fractionation of these magmas led to the development of gabbroic rocks that make up the top of the succession. The Waterberg Project is located in the Southern Marginal Zone of the Limpopo Belt. This position in a structurally active area may have facilitated the creation of space for initial magmas.

It is argued, that the ~~Waterberg succession~~mafic to ultramafic succession of the Waterberg Project does not represent a simple marginal extension of the Aurora Project of the Northern Lobe, nor does it directly correlate with the Platreef. It shares geological features, but represents a separate magmatic basin.

The conclusion that the ~~WB~~Waterberg Succession does not represent a simple strike extension of the Northern Lobe is excellent news for explorers of the Bushveld Complex. ~~and~~It demonstrates, that cooperation of industry and academia, aided by 21st century geophysical techniques, ~~that mineralized successions with their own metal budgets~~ can lead to significant discoveries in well-explored terrains.

1 Introduction

The Northern Lobe of the Bushveld Complex hosts the Platreef and its~~includes the~~ world-class ore bodies. ~~hosted by the Platreef and its~~The stratigraphy and mineralization of the Northern Lobe has been the topic of many studies in recent years. In the light of the discovery of Main Zone-hosted mineralization in the far north and south of the lobe (Harmer et al., 2004; Maier and Barnes, 2010), the Main Zone of the Bushveld Complex is now the center of ~~renewed attention~~exploration. The Waterberg Project is located north of the Northern Lobe and represents a large, recent PGE discovery (Huthmann et al., 2016; Kinnaird et al., 2017). ~~In this publication data for the Waterberg Succession is presented, which in a recent publication McDonald et al. (2017) has been interpreted to be (at least in parts) the lateral equivalent of aforementioned Main Zone-hosted PGE occurrences.~~

The significant Waterberg ~~Pd/Pt deposit~~Pd-Pt mineral system is a >3.5 by 24 km, mafic to ultramafic, lobate intrusion hosting an indicated resource of 24.9 million ounces 4E (Pt+Pd+Rh+Au; 2.5 g/t cut-off) in ~~an~~ upper (T Zone) and lower (F Zone)~~(T and F Zone, respectively)~~ mineralized zones. ~~The~~Its U/Pb ages of 2059 ± 3 and 2053 ± 5 Ma (Huthmann et al., 2016) ~~for the succession~~ overlap within error with the ~~age~~2.06 Ga age (Scoates and Friedman, 2008; Scoates and Wall, 2015; Zeh et al., 2015) ~~s for the~~of the Bushveld Complex. ~~Kinnaird et al., (subm.)~~Kinnaird et al. (2017) provide an extensive overview of the local geology, the relationship of the succession with its roof rocks, and details of the ~~two~~T and F mineralized zones. In this contribution, the stratigraphy of a small area, hosting ~~what by Platinum Group Metals is referred to as a~~ the Super F mineralized zone is described in detail. ~~The geology of the overlying units is described in less detail and the reader is referred to the aforementioned upcoming publication.~~

Drill ~~intercepts~~data from >100 drill holes indicate ~~often~~the presence of discontinuous and variable lithologies in the study area. ~~For~~In this study, a range of drill holes has been logged in detail and ~~below~~ whole-rock major and trace element geochemistry as well as ~~and six element~~ PGE ~~data have been~~are compared to ~~available~~ company assays. The data gathered for this study is used to present the first conceptual model for the evolution of the Waterberg Succession. ~~and i~~It is argued, that ~~if all aspects are considered,~~ the succession does not correlate directly with units described in the southern half of the Northern Lobe of the Bushveld Complex. Possible correlations ~~to~~with ~~units~~the geology at the Aurora Project (Harmer et al., 2004) immediately to the south are explored in detail in the discussion section.

2 Geology

The 2.06 Ga (Scoates and Friedman, 2008; Scoates and Wall, 2015; Zeh et al., 2015) Bushveld Complex is the largest layered intrusion on Earth and the world's largest repository of ~~magmatic~~PGE, Cr and V ~~ore deposits~~ (Lee, 1996). It ~~was traditionally~~is believed to consist of 5 lobes with an estimated areal extent of approximately 65 000 km^2 (Willemse, 1969).~~, however t~~The intersected ultramafic-mafic rocks at the northern end of the Northern Lobe and recent geophysical studies, however, increase this total areal extent to >90 000 km^2 (Finn et al., 2015). ~~While~~Although the lobes were historically interpreted to be separate bodies, more recent ~~re-~~interpretation of the gravity data allows for the possibility that the Eastern and Western Lobes ~~may be~~ connect~~ed~~ at depth (Webb et al., 2004; Finn et al., 2015). Links between the Northern Lobe and the Eastern and Western Lobes are contentious (Cawthorn and Webb, 2001), and links between ~~the~~ the

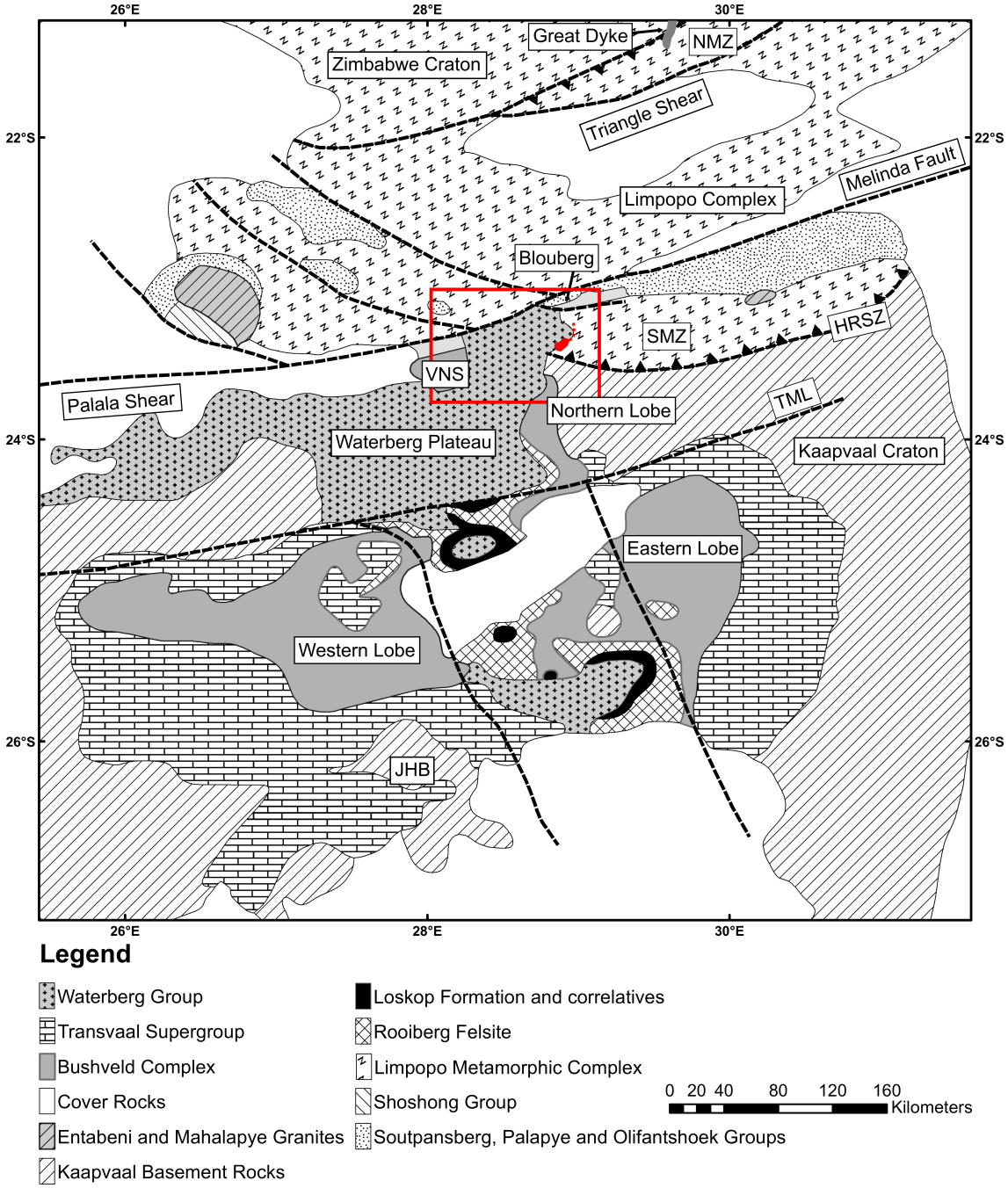

Figure 1: Map showing the distribution of major lithological units in northern South Africa. JHB Johannesburg; SMZ Southern Marginal Zone; NMZ Northern Marginal Zone; TML Thabazimbi-Murchison lineament; HSRZ Hout River Shear Zone. The small rectangle indicates the Waterberg area. Modified after Dorland et al., 2006.

Northern Lobe and ~~mineralized rocks at its northern end~~the Waterberg Project remain to be established ~~and will be discussed in this contribution~~. The controversy also includes the gently south-dipping Villa Nora Segment (Fig. 1) and its relationship to both the Northern Lobe and the ~~mafic succession~~Waterberg Project.

The Bushveld Complex comprises heterogeneous, predominantly felsic volcanics, a mafic to ultramafic suite of 7-8 km thickness, ~~plus~~ a granite as well as a granophyre suite (von Gruenewaldt et al., 1985). The mafic package, also known as the Rustenburg Layered Suite, is subdivided into

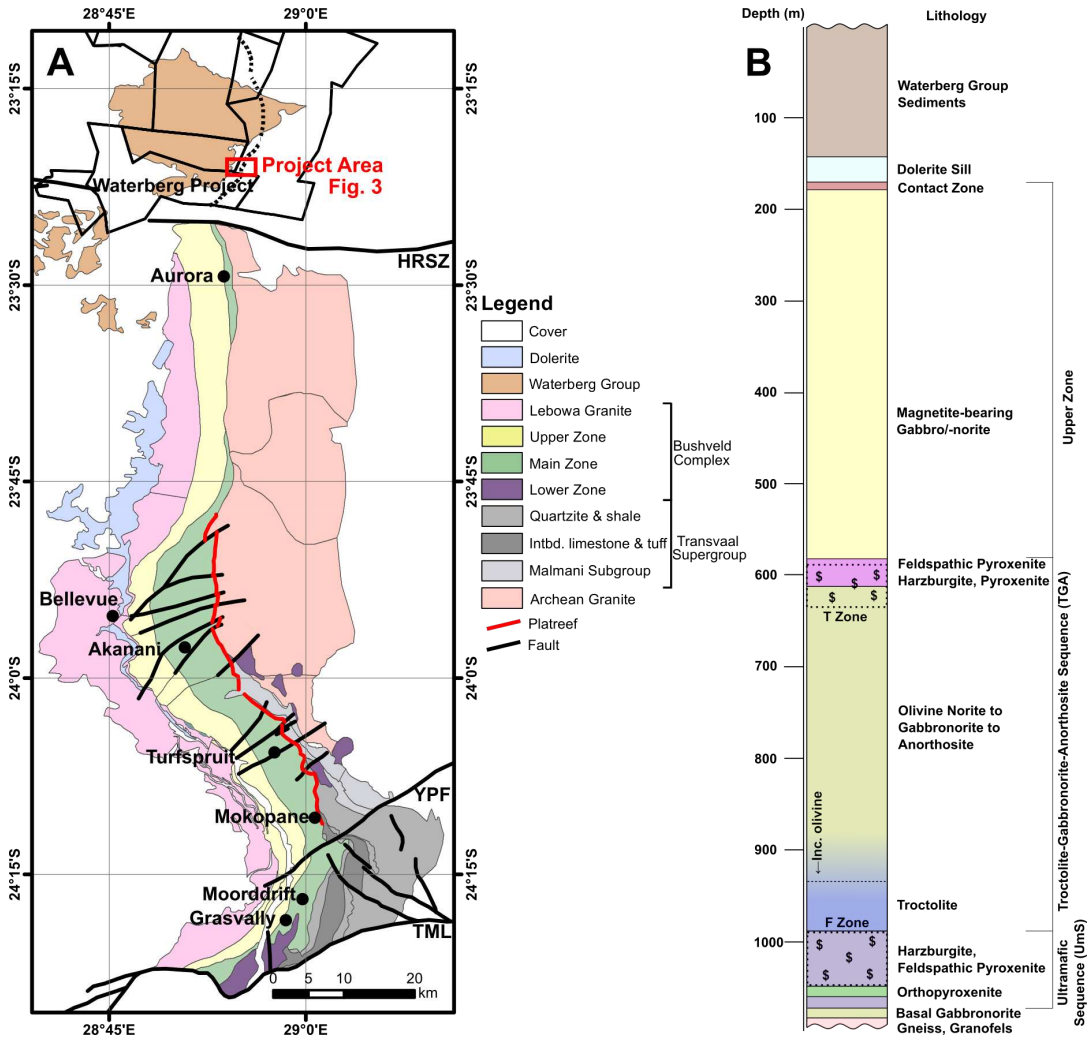

Figure 2: A: Geological map of the Northern Lobe of the Bushveld Complex showing the town of Mokopane and selected mining and exploration projects. HRSZ Hout River Shear Zone; YPF Ysterberg-Planknek Fault; TML Thabazimbi-Murchison lineament. Red Rectangle highlights the area of interest. B: Simplified stratigraphic column for the Waterberg succession. Both the basal gabbronorite and the pyroxenite may not be present or occur at varying position and with varying thickness in the Ultramafic Sequence.

the noritic Marginal Zone, the Lower Zone comprising pyroxenites and harzburgites, the cyclical Critical Zone of chromitite–norite–pyroxenite, the Main Zone comprised of gabbronorites and the Upper Zone of anorthosite, gabbro and magnetitite. Lateral facies variations are common and not all zones are always present (Eales and Cawthorn, 1996; McDonald and Holwell, 2011). The Bushveld Complex is the world's most significant source of platinum group elements including gold and chromite, as well as a source of magnetite and ilmenite (Lee, 1996).

2.1 The Northern Lobe and the Platreef

The geology of the Platreef and Northern Lobe are reviewed in great detail in Kinnaird et al. (2005), Ashwal et al. (2005), Kinnaird et al. (2005), McDonald and Holwell (2011) and Kinnaird and Nex (2015). and only aspects relevant to this contribution are discussed .An overview of the geology relevant for the discussion of the Waterberg Project is provided by Kinnaird et al. (2017).

The succession of mafic to ultramafic rocks in the Northern Lobe differs from the Eastern and

Western Lobes, ~~however~~but all zones can be recognized. The Lower Zone was emplaced in trough-like depressions and is characterized by high-Mg ~~whole-rock composition~~rocks, chromitites and zones of Ni-PGE mineralization ((Hulbert and von Gruenewaldt, 1982, 1985; Yudovskaya et al., 2013b, 2017)~~, Yudovskaya et al., subm.)~~. ~~It~~The Lower Zone is separated from the Platreef by older Transvaal sediments or granite gneisses. The ~~predominant~~main basal unit is the Platreef, a pyroxenite-dominated, lithologically variable unit irregularly mineralized with PGE~~,~~ and Ni~~,~~ and Cu sulfides. It onlaps northwards onto progressively older Transvaal metasedimentary units of oxide facies iron formations and dolomite and eventually onto Archean granites and gneisses (Kinnaird et al., 2005). The Platreef disappears approximately half-way along the Northern Lobe. ~~It is unconformably overlain by the Main Zone.~~ Data from Turfspruit confirms a general westward dip of 30° to 60° close to surface, the dip however lessens with depth into a more regularly layered sequence (Grobler et al., 2012; Yudovskaya et al., 2017). The Platreef is considered to be the stratigraphic equivalent of the Critical Zone and unconformably overlain by the <2000 m thick Main Zone. Overlying the Main Zone, the Upper Zone of the Northern Lobe is marked by the first occurrence of massive magnetitite (van der Merwe, 1976). The Upper Zone is transgressive and overlies Main Zone for most of the strike length of the Northern Lobe, although in the north it is in direct contact with a basement high (Fig. 2A). This basement high separates what might be a southern magmatic basin comprising the Platreef, and a northern magmatic basin comprising the Aurora mineralization (Kinnaird et al., 2005; McDonald et al., 2017). In the Bellevue drill core (Fig. 2A), the Upper Zone comprises 1200 m of predominantly magnetite-rich olivine gabbro and olivine ferrodiorite (Ashwal et al., 2005).

Correlations between the Eastern and Western Lobes and the Northern Lobe are complicated by the enigmatic ~~t~~Troctolite ~~horizon~~Marker, ~~a c.~~which is a ~110 m thick package of noritic troctolite located 1100 m above the base of the Main Zone~~ located~~ along 35 km ~~of~~ strike length in the central south of the Northern Lobe~~of the Main Zone~~ (van der Merwe, 1976). Very little olivine occurs in the Main Zones of the Eastern and Western Lobes (Eales and Cawthorn, 1996) and recent ~~findings~~research suggest that the ~~horizon~~Troctolite Marker may be prospective for PGE exploration (Tanner et al., 2014). ~~In contrast to the Eastern and Western Lobes, t~~The Main Zone of the Northern Lobe has an erosional contact at its base and is interpreted to significantly postdate the emplacement of the Platreef (Holwell et al., 2005; Holwell and Jordaan, 2006). Rather than being involved in the formation of the Platreef-equivalent Critical Zone deposits in the Eastern and Western Lobes, the Main Zone of the Northern Lobe may therefore have retained its PGE budget (Kruger, 2005; Seabrook et al., 2005)~~. rather than being involved with the formation of Critical Zone deposits (Kruger, 2005; Seabrook et al., 2005) and hence may have retained its PGE budget.~~ ~~While~~Whereas most of the economic value of the Northern Lobe is concentrated in the Platreef, sub-economic mineralization has been intersected in rocks interpreted to belong to the Main Zone in the far north at Aurora and south at Moorddrift (Fig. 2A; Harmer et al., 2004; Manyeruke, 2007; Maier et al., 2008; Maier and Barnes, 2010; McDonald and Harmer, 2010; Holwell et al., 2013; McDonald et al., 2017). ~~Overlying the Main Zone, the Upper Zone of the Northern Lobe is marked by the first occurrence of massive magnetitites (van der Merwe, 1976).~~

~~While generally overlying the Main Zone, the Upper Zone does directly overly a basement high in the northern part of the lobe, separating what might be called a southern "basin" with the Platreef and a northern "basin" with the Aurora mineralization (Kinnaird et al., 2005).~~

The Platreef is one of the world's largest and most valuable ~~sequences~~ mafic to ultramafic successions ~~of~~comprising platinum-group elements and associated significant Ni and Cu reserves (Naldrett, 2010). It differs from the UG2 and Merensky Reef deposits of the main Bushveld Complex

in terms ~~of thickness of the package~~of being thicker, having lower average Pt/Pd ratios of approximately 1 and lower grade of >4 g/t PGE where mined (Kinnaird et al., 2005). PGE and base metal sulfides are generally associated, however in detail they may be decoupled, possibly due to hydrothermal alteration and local remobilization (Kinnaird et al., 2005; Holwell and McDonald, 2006). A recent age date for the Platreef of 2056 ± 5 Ma (Yudovskaya et al., 2013a) overlaps within error with ~~a~~ precise ~~2055 Ma~~2056.88 ± 0.41 Ma and 2057.04 ± 0.55 Ma ages for the Merensky Reef (Scoates and Wall, 2015) and indicates that both deposits formed broadly contemporaneously. These ages are also in agreement with high-precision U-Pb dating ~~indicating~~that indicates crystallization of ~~that~~ the ~~whole~~ Bushveld Complex ~~crystallized within~~over 1 Ma (Zeh et al., 2015).

Mineralization south of Mokopane at Moorddrift (Maier and Barnes, 2010), ~~in~~ the Aurora Project (Harmer et al., 2004; Manyeruke, 2007; Maier et al., 2008; McDonald and Harmer, 2010; McDonald et al., 2017) ~~in the north of the Northern Lobe~~ and ~~in the~~the Waterberg Project ~~(~~(Kinnaird et al., 2014; Huthmann et al., 2016; Kinnaird et al., 2017)~~; Kinnaird et al., subm.)~~ ~~is~~is explicitly excluded from the Platreef (Kinnaird et al., 2005; McDonald and Holwell, 2011). The Aurora Project is interpreted to be an upper Main Zone-hosted Cu-Ni-PGE deposit (McDonald et al., 2017) located to the south of the Waterberg Project ~~in~~at the very northern end of the Northern Lobe (Fig. 2A). At Aurora, the Main Zone reappears at surface and is in direct contact with Archean granite. Mineralization occurs in two main mineralized horizons and a thinner discontinuous horizon closer to the basal contact.

The Northern Lobe is separated from the Bushveld by the Thabazimbi-Murchison-Lineament. The TML is a 500 km long and 25 km wide, ENE-WSW striking, long-lived and repeatedly reactivated craton-scale structure (Good and de Wit, 1997). Based on seismic anisotropy, the TML is interpreted to represent a fundamental crustal and possibly deep lithospheric mantle ~~break~~lineament within the Kaapvaal craton. ~~that~~It is thought to have influenced regional stresses and tectonically induced fluid flux during its reactive history between 2,960 and 145 Ma (Good and de Wit, 1997 and references therein). The stratigraphic correlation between the Northern Lobe to the north and Eastern and Western Lobes to the south of the TML remains contentious (van der Merwe, 1976; Ashwal et al., 2005; Kruger, 2005; McDonald et al., 2005; Kinnaird and Nex, 2015).

The Hout River Shear Zone (Fig. 2A) marks the boundary between the granulite-facies Southern Marginal Zone (SMZ) of the Limpopo Complex and the ~~stable~~ Archean Kaapvaal Craton. ~~and~~ It is generally interpreted to represent a composite structure along which the Southern Marginal Zone was thrust southward during the Neoarchean (Smit et al., 1992; Barton et al., 2006). According to recent work by Nicoli et al. (2015), the SMZ consists of reworked Kaapvaal Craton basement gneisses, mafics, and clastic sedimentary rocks with ages between 3.3 and 2.7 Ga which are overlain by younger sedimentary rocks~~s~~. There is still little consensus regarding some elements of the geodynamic history of the Limpopo orogeny (e.g. Treloar et al., 1992; Holzer et al., 1998; Barton et al., 2006; Nicoli et al., 2015), however, a N–S directed long-lived tectonothermal activity of more than 700 Ma is well established (Kramers and Mouri, 2011). Several studies (Schaller et al., 1999; Barton et al., 2006; Clarke et al., 2009; Smirnov et al., 2013; Rajesh et al., 2014) proposed a Paleoproterozoic (and not Archean) collision of the Zimbabwe and Kaapvaal craton that may account for certain geological features observed in the project area. Regardless of the timing of the Limpopo Belt orogeny, the location of the Waterberg Succession in the SMZ (~~instead of~~not the Kaapvaal Craton) may expose it to a level of Paleoproterozoic tectonism that ~~can~~is not generally ~~be~~ observed in the undeformed Bushveld Complex.

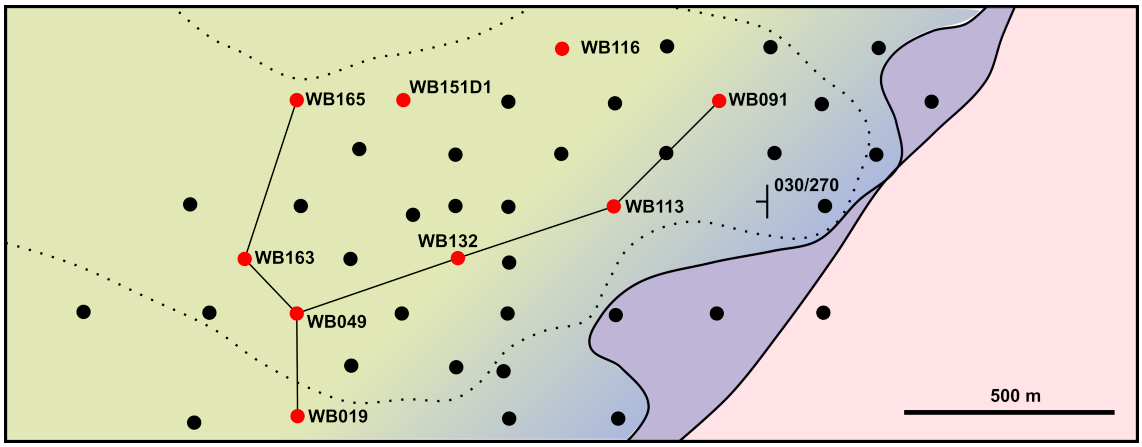

Figure 3: ~~Close-up~~Subcrop map of the area ~~of interest~~ shown in Fig. 2. Shown are the positions ~~It displays the relative positions~~ of the drill holes investigated in detail (red) and the cross- and long-section ~~drawn~~from Fig. 13 and 14. The ~~S~~stippled line~~s~~ ~~show~~marks the approximate outline of a 1 g/t 3E grade shell projected to surface. It has a 30 dip to the west. The sedimentary rocks overlying the succession are approximately 240 m thick in the east and their thickness increases slightly to the west. ~~Shading indicates the changing depth of basement intersect from c. 600 m in the east to almost 1200 m in the west. Grid is 500 x 500 m N-S.~~

2.2 Local Geology

In the area immediately north of the Hout River Shear Zone (Fig. 2A) Platinum Group Metals (PTM) has intersected a mafic to ultramafic succession ~~consisting~~subdivided into ~~of~~ an Ultramafic Sequence (UmS) overlain by ~~what is now referred to as~~ the Troctolite--Gabbronorite--Anorthosite Sequence (TGA) and an Upper Zone (UZ) of magnetite-bearing gabbroic rocks to ferrogabbros. The rocks ~~are~~ rest~~ing~~ on a footwall of Archean gneisses that is commonly interfingered with pyroxenite (Fig. 2B). Except for one drill hole in the very south of the prospect, calc-silicate xenoliths are absent in the Waterberg area. Early pyroxenitic magmas intruding the floor rocks caused ~~a~~ melting and subsequent mingling of the ~~two components~~pyroxenitic magma and granitic melt, leading to the formation of a granofels. These earliest intrusion are envisioned as tube-like or chonolithic conduits that with subsequent intrusions were assimilated or broadened. The igneous ~~rocks~~package of rocks ~~are~~ dips~~ping c.~~ $\sim 30^\circ$ toward the west-northwest, with variations ~~due~~because ~~to~~of structural controls and/or ~~channel formation~~thermal-mechanical erosion. Significant faults are indicated by variations in intersection depth of the sedimentary-igneous rock contact, however, due to vertical drilling these potential steeply-dipping structures are not typically intersected.

Recent geophysical modeling suggests a continuation of the mafic succession to the north and west of the drill intersections and a greatly increasing thickness towards the southwest (Finn et al., 2015). The subdivision of the stratigraphy has changed since the early years of exploration and the ongoing work by company geologists and academics involved with this project has ~~led to the~~ question~~ing~~ed ~~of~~ some ~~arrangements~~relationships (e.g. in Huthmann et al., 2016) and prompted a new subdivision to reflect interpreted petrogenetic relationships (Kinnaird et al., 2017).

The base of the succession ~~may~~sometimes comprises very fine- to fine-grained orthopyroxenites and/or gabbronorites. Orthopyroxenites occur as cm- to meter-sized fragments to sill-like bodies that have sharp to gradational contacts with their respective host rocks and in places are almost completely assimilated by subsequent ultramafic rocks (see below). Gabbronorites generally appear less affected by their host and their relative age is uncertain. The pyroxenites are interpreted to be the crystallization product of initial ~~liquid~~magmas ~~to~~ intrude~~ing~~ the area and based on drill

intersects outside of the study area may intrude >100 m into the footwall granite-gneisses. Due to very limited drilling into the deep basement, their distribution ~~however~~ is not certain.~~ and b~~Based on the observed degree of assimilation and their distribution, they may also represent autoliths. The gabbronorites, on the other hand, are plagioclase-dominated rocks of varying grain-size (finer-grained towards the footwall) that ~~in thin section~~ resemble the geology of gabbroic rocks observed higher up in the succession.

Harzburgites and feldspathic pyroxenites of the UmS are the primary basal unit of the succession. ~~Where present~~The UmS is discontinuous and where present~~, the package~~it may exceed 80 m in thickness, hosts PGE and Au mineralization and unevenly distributed chromite clusters and seams. Olivine-bearing units in the UmS are very strongly altered with ~~often only~~ relicts of primary minerals remaining, having been replaced primarily by serpentine and magnetite. ~~Calc-silicates are absent, however t~~The unit is very heterogenous and comprises small amounts of juxtaposed pyroxenite, serpentinite, troctolite and dunite. Calc-silicates xenoliths are absent.

Overlying the UmS, the TGA Sequence is primarily composed of gabbronoritic rocks with minor anorthosites, grading into norites, olivine norites and troctolites at ~~its~~the base (Fig. 2B). The rocks appear to ~~be~~ grad~~ing~~e into the UZ at the top of the succession. ~~and d~~Due to the fine-grained nature of the magnetite and similarity of rock types, no clear contacts can be observed. The enigmatic troctolites~~, which are dissimilar to any ultramafic Bushveld units,~~ have a gradational, mingled or irregular contact with olivine gabbronorite upwards and a sharp, erosional(?) contact with harzburgite at the base (Fig. 4B). Further south, the top of the TGA Sequence is host to the T Zones, a set of 2 to 3 discontinuous, mineralized gabbronorite~~ic~~, pyroxenit~~ic~~e to troctolit~~ic~~e, ~~discontinuous, mineralized~~ horizons. In the area of focus for this study the T Zones are either absent or extremely poorly developed, possibly related to non-deposition, structural controls, or erosion preceding the deposition of Waterberg Group sediments.

The upper part of the succession on the Waterberg Prospect is composed of magnetite-bearing gabbronorite and gabbro~~,~~ that ~~contain~~have varying ortho- and clinopyroxene content~~s~~. It is tentatively correlated with the Upper Zone elsewhere in the Complex, even though it lacks the magnetitite layers ~~which~~that are characteristic for the Upper Zone elsewhere in the Bushveld Complex (e.g. Molyneux, 1974; Ashwal et al., 2005). Instead, magnetite in the Upper Zone at the Waterberg Project occurs as very fine-grained disseminations that in the field are most easily identified by the use of a magnetic susceptibility meter. The UZ thins in places and its exact distribution requires further research~~ and may be controlled by structure-controlled blocks and erosion~~. ~~The absence of distinct magnetitite layers and more evolved apatite-bearing rocks may be related to erosion of more evolved units rather than non-deposition.~~

The top contact of the Waterberg Succession is a remarkably flat erosional unconformity overlain by Paleoproterozoic Waterberg Group sediments (Callaghan et al., 1991; Huthmann et al., 2016), typically starting with a coarse, poorly-sorted~~basal~~ and polymict breccia. The top of the succession is complex and sometimes an up to 10 m wide and strongly altered, sheared and tuffaceous contact zone is located between the sediments and igneous units. Detrital zircons of the basal breccia have recently been dated and encompass age clusters of 2045 to 3354 Ma, generally attributed to the Limpopo Belt (Corcoran et al., 2013; Huthmann et al., 2016).

Recently acquired age dates (2059 ± 3 and 2053 ± 5 Ma; Huthmann et al., 2016) from zircons extracted from mafic rocks of the succession are within error coeval with published ages for the Eastern and Western Lobe of the Bushveld Complex (Walraven and Hattingh, 1993; Walraven, 1997; Buick et al., 2001; Scoates and Friedman, 2008; Scoates and Wall, 2015; Zeh et al., 2015),

and the Northern Lobe (Yudovskaya et al., 2013a), ~~and suggest~~ which indicates that the intrusions ~~are related~~belong to the Bushveld Large Igneous Province and are therefore related.

Mineralization occurs in ~~two mineralized zones~~the T and F zones, located just below the Upper Zone and in the Ultramafic Sequence, respectively (Fig. 2B). The ~~The so called T and F Zones~~mineralized zones are 3 to >60 m thick and have so far been intersected along 17 km of strike (Kinnaird et al., 2014). T and F Zone refers to zones of elevated PGE grades which in detail are not not strictly stratabound (2B). The T Zone in particular occurs in two distinct stratigraphic levels with distinct mineralogy (Kinnaird et al., 2017). New mineral assemblages are still being discovered and will be subject of upcoming publications. The mineralized F Zone closely follows the westerly trend of the harzburgite chonoliths and may form "Super F Zones" with grades that can exceed 15 g/t 3E (Pt+Pd+Au) in individual assayed intervals ~~and that have no direct analogue in the Bushveld Complex~~ (Kinnaird et al., 2017). These zones of high grade are separated by weakly to ~~non-~~unmineralized ~~rocks~~troctolite of the TGA Sequence.

3 Methodology

For this study drill core from nine holes intersecting the center and periphery of one of the Super F (mineralized) Zones (Fig. 3) have been logged. The selected drill holes allow for an assessment of any correlation of rock types, distribution of the mineralization and ultimately the generation of an emplacement model. This particular Super F Zone forms an elongated, SW-plunging mineralization envelope of >200 by >1000m with ~~highly~~ anomalous PGE and Au of greater 0.5 g/t ~~values~~ over more than 120 m in core and economic grade of over 2.5 g/t over more than 60 m. ~~PTM's~~Platinum Group Metal's assay database for the study area, consisting of approximately 9500 assays of Pt, Pd, Ni, Cr, Cu, Co and S, ~~assays~~ was made available. Figures 13 and 14 show typical long and cross sections through this zone and assays ~~as per~~derived from PTM's database.

Fifty-eight samples of approximately 25 cm long, NQ size, quarter-core samples were selected from the logged drill holes. Care was taken to avoid zones of veining, strong alteration and autoliths/xenoliths. Sample preparation was conducted at the University of Witwatersrand following established methods (Wilson, 2012).

All samples were analyzed for major and trace elements and loss on ignition (LOI) at the University of the Witwatersrand analytical facilities. Major and selected trace elements were determined using a Panalytical PW2404 X-ray fluorescence (XRF) spectrometer with fused disks and the SuperQ program. Sulphur was determined for selected samples from pressed pellets employing the same instrument and the ProTrace program. All other trace elements were determined by inductively coupled plasma mass spectrometry (ICP-MS) employing a Perkin Elmer Elan instrument. All analytical procedures followed the methods described by Wilson (2012).

Platinum group elements and Au were determined for selected samples at Cardiff University from 15g sample weight powders prepared at the University of the Witwatersrand. The analysis was carried out by Ni-sulphide fire assay followed by Te co-precipitation and ICP-MS (Huber et al., 2001; McDonald and Viljoen, 2006). Accuracy for all whole-rock geochemistry was constrained by the analysis of certified international reference materials and internal standards while the precision for fire assays was estimated by repeat analysis of several samples (see supplementary data).

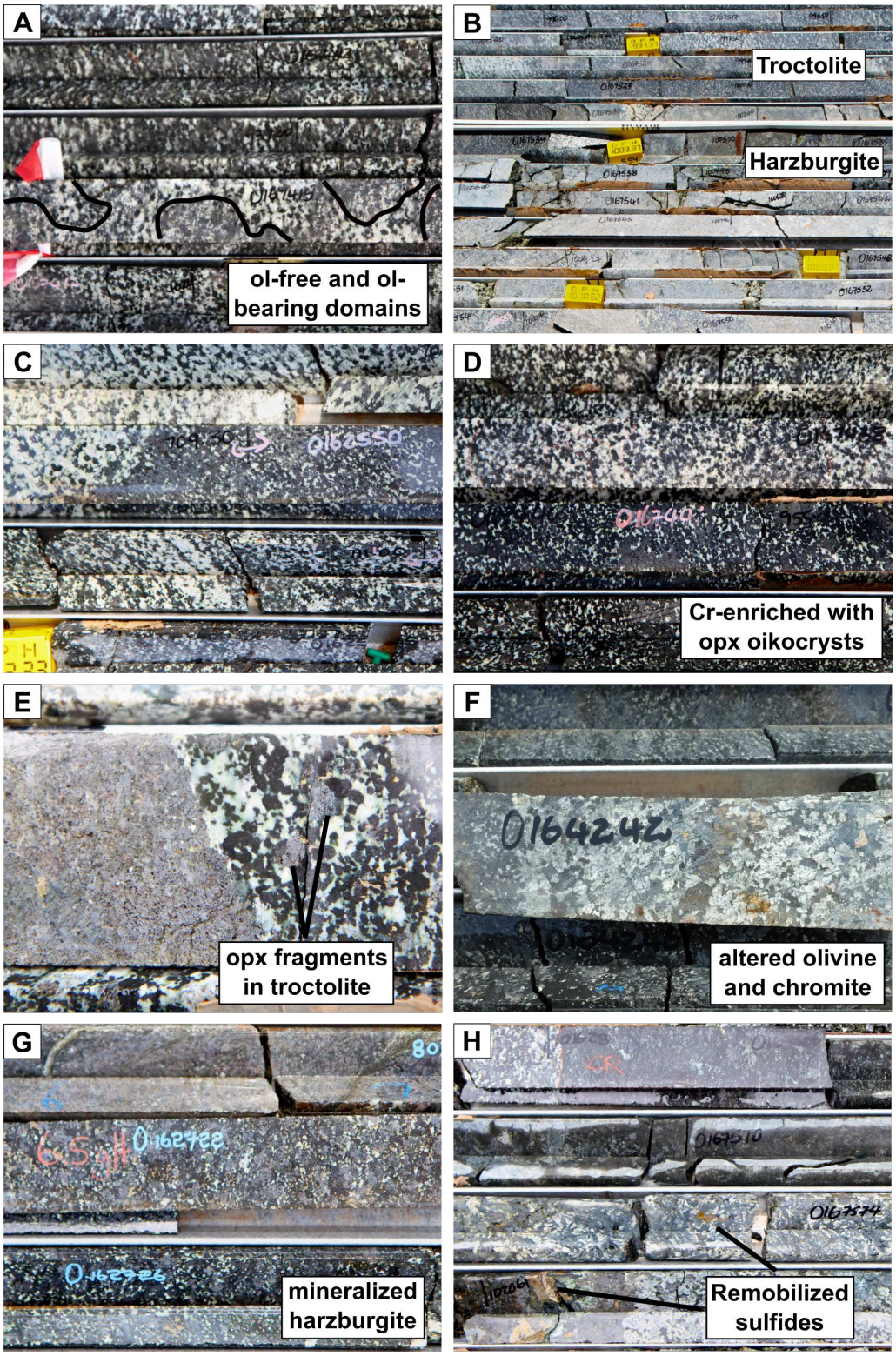

Figure 4: Texture~~s~~al relationships in examples of rock types from drill core ~~observed~~ in the Waterberg ~~core~~Project. A: Upper contact of the TGA Sequence troctolite showing discrete zones of gabbroic and troctolitic rocks interpreted to represent mingling of cumulates; B: Typical Ultramafic Sequence. In the top tray the sharp contact between overlying troctolite and harzburgite is visible; C: Variations in the troctolite zone showing leucotroctolite and zones of abundant orthopyroxene oikocrysts; D: Variations in olivine abundance in the troctolite zone. The oikocryst-rich melatroctolite is characterized by significant spikes in Cr content; E: Orthopyroxenite autolith in troctolite. Note the small pyroxenite fragments in the troctolite and the presence of possibly remobilized sulfides in both rocks; F: Chromite in TGA Sequence troctolite adjacent to an alteration halo and remobilized sulfides; G: Mildly altered mineralized zone with 6.5 g/t Pt+Pd+Au; H: Vari-textured zone of Cr-enriched serpentinite and ~~large~~ sulfide ~~blebs~~remobilization.

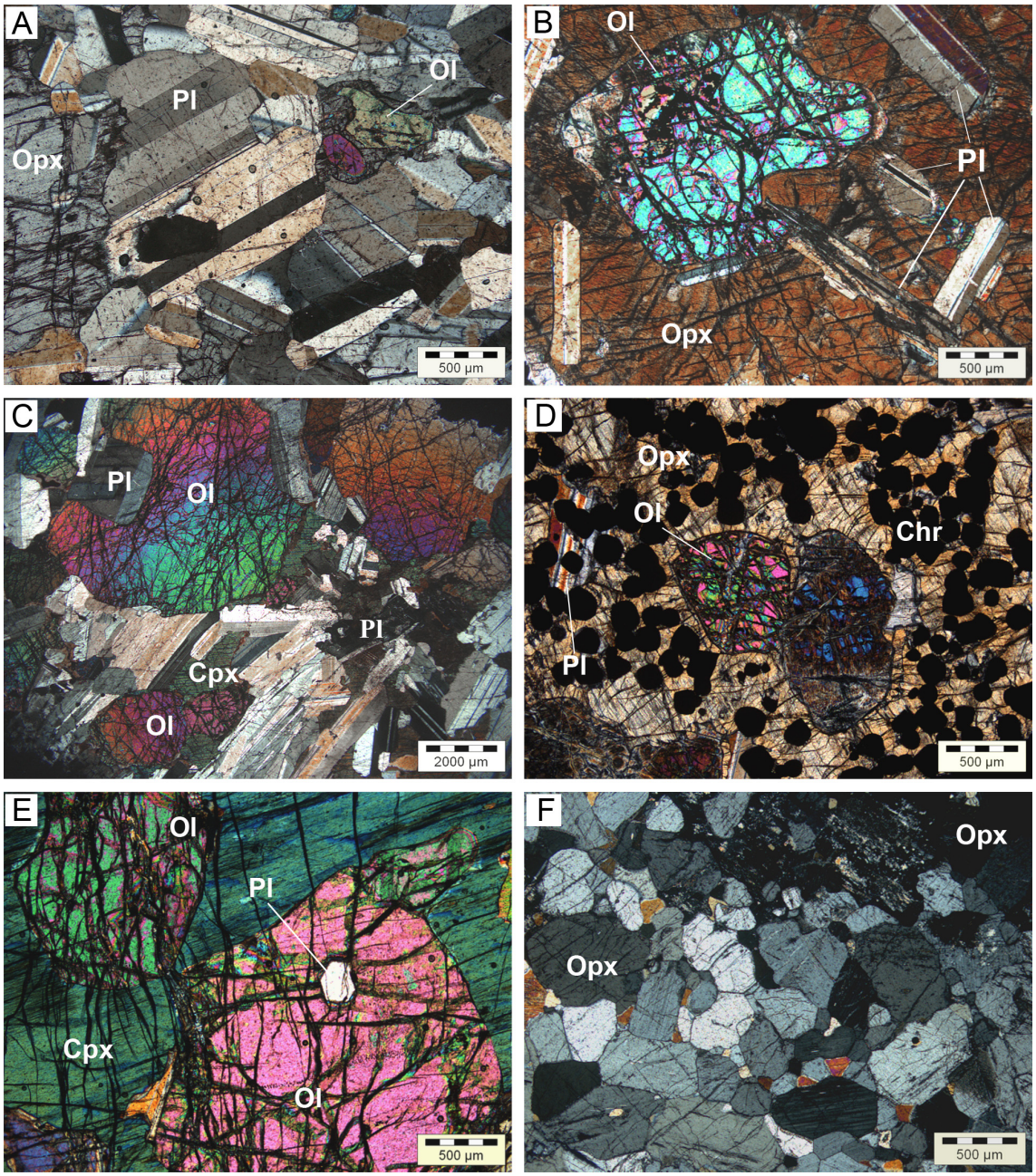

Figure 5: Rock textures of the Waterberg body under cross-polarized transmitted light. A: Small olivine crystals rimed by peritectic orthopyroxene in olivine-bearing leuconorite in the uppermost part of the TGA Sequence; B: Corroded olivine and euhedral plagioclase laths in orthopyroxene oikocryst in olivine norite; C: Coarse olivine and plagioclase of smaller size in troctolite; D: chadacrysts of olivine and chromite enclosed by orthopyroxene in poikilitic chromitite of the Ultramafic Sequence; E: Coarse grains of olivine with plagioclase inclusions among interstitial clinopyroxene in lherzolite of the Ultramafic Sequence; F: Recrystallized orthopyroxenite with triple junction texture of orthopyroxene grains.

4 Results

4.1 Field relationships and petrography

Given the very heterogeneous and irregular nature of lithologies observed in drill core, ~~complexities of the Waterberg area and the high probability of non-sequential intrusion of cumulates, some of~~

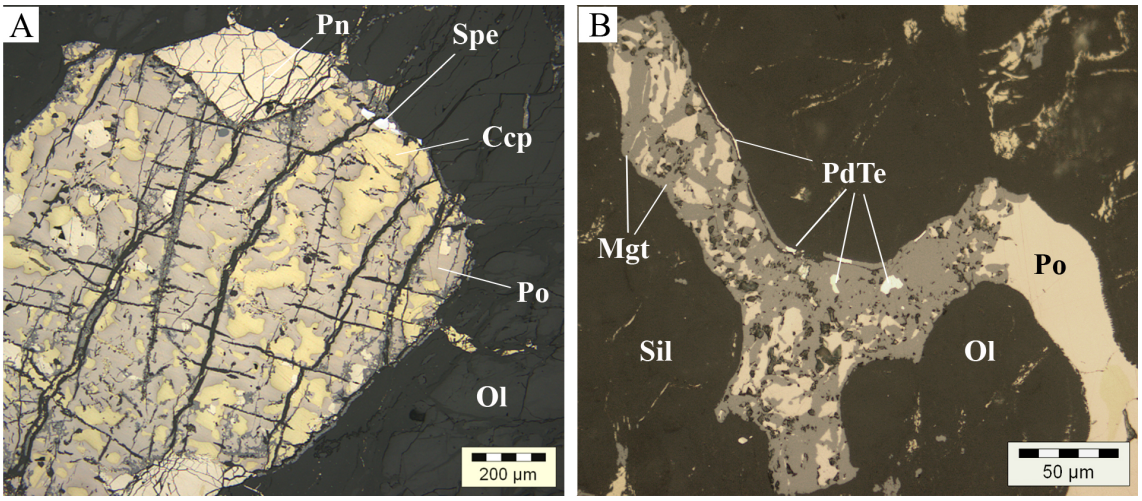

Figure 6: Sulfide assemblages of the F Zone under reflected light. A: Primary magmatic sulfide bleb composed of pentlandite (Pn), pyrrhotite (Po) and chalcopyrite (Ccp) in harzburgite. Sperrylite (Spe) occurs at the margin on contact with olivine (Ol); B: Interstitial pyrrhotite partly replaced by secondary magnetite (Mgt) in harzburgite. Kotulskite (PdTe) is located inside magnetite and remobilized along the contact between sulfides and silicates (Sil). Olivine is completely replaced by serpentine.

~~the complexities have been simplified and~~ we discuss suites of intrusives and zones of mineralization rather than individual lithologies ~~are discussed~~ (cf. McDonald and Holwell, 2011). It has to be emphasized, that ~~while~~although individual rock types are important, the amount of variation in mineralogy, alteration, chemistry and mineralization makes lithological correlation between 200 m-spaced drill holes ~~incredibly~~ difficult ~~on a lithology level~~. The variation in mineralogy observed in the core may be related to mingling and mixing of crystal-rich liquids. The term mixing is used in situations where two or more magmas produce hybrid rocks with the identities of the parent magmas obscured, whereas mingling represents interactions in which the original magmas or cumulates retain their identity (Fig. 4; Wiebe, 1980). ~~As outlined earlier, the succession is subdivided into Upper Zone (poorly developed in the study area), Troctolite-Gabbronorite-Anorthosite Sequence and Ultramafic Sequence.~~

In accordance with informal tradition amongst Bushveld Complex geologists, rock types are named based on their cumulus mineralogy, hence a rock consisting of cumulus olivine and plagioclase with significant intercumulus orthopyroxene is called a troctolite rather than a olivine norite. The term reef is avoided in favor of mineralized zone, as reef implies a lateral continuity that may not be present in the Waterberg Succession. Additionally, the mineralization may to a limited degree transgress ~~rock type boundaries to a limited degree.~~boundaries between rock types.

The following section provides drill core and petrological observations for the four main lithologies of the study area, namely the basal orthopyroxenite and gabbronorite, as well as the Ultramafic Sequence (UmS) and Troctolite-Gabbronorite-Anorthosite Sequence (TGA).

4.1.1 ~~Marginal~~Basal orthopyroxenite

Orthopyroxenite occurs as sill-like bodies and as autoliths throughout the ~~lower part~~Ultramafic Sequence and more rarely in the troctolite ~~–~~ of the TGA Sequence~~of the succession, generally in troctolites and harzburgites~~. Outside the area investigated as part of this study, orthopyroxenites may intrude deep into the footwall, however, due to limited drilling into the basement, ~~its~~their

detailed distribution is not well ~~resolved~~established. The autoliths are several centimeters to <6 m in size. Their ~~with generally well recognizable~~ contacts are generally well-recognizable, but particularly in harzburgite may be obscured by alteration.~~which may be obscured by alteration, particularly in the harzburgites.~~ The rocks consist of medium to very fine-grained orthopyroxene and may contain up to 15% olivine. Clinopyroxene and plagioclase are minor interstitial phases. Both orthopyroxene and olivine may host disseminated crystals of chromite which range in size from <50 μm to <10 μm. The smallest of those crystals may form trails in the host silicate.

The orthopyroxenites are barren, or, where their texture suggests sulfide remobilization into the rock, contain ~~low~~trace 3E (Pt+Pd+Au) ~~grade~~levels. Inspection of the drill cores~~-~~ indicates that ~~that where Cr is elevated in the assays, lithologies are often orthopyroxenites or orthopyroxene-rich~~intervals of orthopyroxenite often have highly anomalous Cr values (Fig. 13 and 14, see below). Core logging also ~~suggests~~indicates that incorporation of these pyroxenites by younger olivine-bearing rocks may lead to zones of increased orthopyroxene oikocrysts ~~-~~or xenocrysts with chromitite clusters.

~~The rocks consist of medium to very fine-grained orthopyroxene and may contain up to 15% olivine. Clinopyroxene and plagioclase are minor interstitial phases. Both orthopyroxene and olivine may host disseminated crystals of chromite. Observed crystals range in size from <50 μm to <10 μm and for the smallest crystals can form trails in the host silicate.~~

Near the granite-gneiss footwall contact, varying amounts of interaction between ~~the rocks~~magmas can be observed~~,~~ and the drill core shows features ranging from discrete felsic and pyroxenitic patches to almost complete homogenization. ~~While~~Although the amount of pyroxenite preserved in the core is often limited to patches of cm-size, a generally decreasing crystal size up hole can be observed. The respective thin sections have small crystal size, triple-junction assemblages of orthopyroxene, and occurrences of quartz-feldspar granophyric intergrowths. Fragments of orthopyroxenite with fine-grained granoblastic texture can be found in ultramafic assemblages, indicating their assimilation by later melt influxes. Together, these observations indicate that the pyroxenite was the first unit to intrude the study area.

4.1.2 ~~Marginal~~Basal gabbronorite

The term marginal gabbronorite is used to refer to occurrences of gabbroic to anorthositic rocks of centimeter to meter thickness found close to the base of the succession. The rocks are very fine- to medium-grained, dark in color and when fine-grained resemble pyroxenites in hand specimen.

Thin sections show that the dark color is due to extensive cloudiness and spotty alteration of plagioclase. The basal rocks exhibit highly variable textures both within a single thin section as well as between different drill cores. Modal mineralogy is dominated by plagioclase with varying amounts of clino- and orthopyroxene. Pyroxene may occur interstitial, as small cumulus crystals or as large oikocrysts. Plagioclase is often altered by very fine-grained mineral aggregates. Overall, in thin section these rocks resemble gabbroic rocks higher up in the stratigraphy.

4.1.3 The Ultramafic Sequence

The mineralized Ultramafic Sequence (UmS) ~~in the project area~~ is a highly complex array of a variety of rock types that includes strongly to very strongly altered harzburgite,~~ troctolite,~~ serpentinite~~ and~~, feldspathic pyroxenite and minor troctolite with very fine to pegmatitic crystal size. It varies in thickness between 60 and >80 m and generally comprises autoliths of orthopyroxenite

which may or may not be altered and which do not contain primary sulfides. Alteration and remobilization appear to have at least some control over the high grade zones and may have affected low grades zones as well (Fig. 4H). Chromite may occur as highly irregularly-distributed seams or clusters of chromite grains that can not be correlated between the widely-spaced holes.

The UmS is the major basal unit of the the Waterberg Succession and can be recognized by its strong alteration and overall heterogenous texture.~~,~~ Its texture ~~which are~~is in sharp contrast to the overlying troctolite's "salt and pepper" appearance~~texture~~ (Fig. 4B). The lower contact of the UmS may be with either with the marginal units, with granofels, or, at the outer margins of the mineralized zone with barren, relatively unaltered meso- to melatroctolite (Figs. 13 and 14). The appearance of ~~an~~the unaltered texture ~~in~~of the troctolite invariably indicates barren zones (Fig. 13, WB113D0), however sulfide remobilization may lead to ~~irregular low grade zones.~~ zones of highly irregular grade (Figs. 4H, 13, WB091D0). Due to this, base metal sulfides can be found highly concentrated and may comprise zones of >10 g/t 3E for individual samples (Fig. 4H bottom). This relationship is not consistent, however, and both base and previous metals may occur separately. Where drill cores suggest interactions of different magmas, base metal sulfides (and associated PGE) may be absent (Fig. 4H top).

~~In thin section t~~The harzburgites are medium- to coarse-grained rocks consisting of about equal proportions of orthopyroxene and olivine. Plagioclase and clinopyroxene are minor interstitial components. Plagioclase may form leucocratic patches of generally finer grain size. Pyroxene and olivine, in particular, are very strongly altered and only the outline of former minerals remains in some cases. The dominant alteration is to serpentine ~~plus~~and magnetite, however, chlorite and a range of other alteration minerals occur. Carbonates or carbonate overprint are not observed. Chromite forms rare small grains in amounts of less than 1 vol%, although it can be found as chromite clusters (Fig. 5) or as irregular seams. Sulfide minerals observed as part of the F Zone mineralization include pentlandite, pyrrhotite and chalcopyrite, often associated with significant secondary magnetite due to the strong alteration of the harzburgites. ~~The~~ P~~p~~latinum group minerals ~~are variable~~ in the T Zone are variable (Fig. 6). ~~with dominant s~~Sperrylite is dominant ~~and~~ and subordinate Pt-Pd bismutho-tellurides, Au-Ag alloys, Pd arsenides and Pt-Rh sulpharsenides can be found.

4.1.4 The T~~GA~~roctolite-Gabbronorite-Anorthosite Sequence

The troctolites in the lower part of the Troctolite-Gabbronorite-Anorthosite (TGA) Sequence form an unmineralized, 50 to 110 m thick package ranging in composition from leucotroctolite and olivine norite to melatroctolite ~~and~~with rare plagiodunite towards the base. The troctolites have a cross-cutting and erosional relationship with underlying harzburgites of the UmS (Fig. 4B). Towards the lower contact, the troctolite typically gradually increases in olivine content and its appearance is more homogeneous. Most of the sequence contains between 50 and 80% olivine, giving it a distinct salt and pepper appearance. Sharp breaks in composition may occur, ~~however,~~ leading to the juxtaposition of rocks of varying olivine content (Fig. 4C). Where developed, the more anorthite-rich phases appear to crosscut and postdate the olivine-rich zones~~, perhaps indicating fractionation~~. The sequence is coarse-grained with rare pegmatitic patches, typically with increased anorthite content. Most of the sequence contains up to 10% orthopyroxene in the form of up to several centimeter-sized oikocrysts. This may increase in the lower half of the sequence to >40%, usually at the expense of plagioclase. The upper 10 to 50% of the sequence may be very heterogeneous in composition and discrete domains of troctolitic and gabbronoritic composition

can be distinguished (Fig. 4A).~~,~~ This is interpreted to indicate the interaction of the respective differentiating crystal-rich liquids.

As with the ~~The~~harzburgite of the UmS, the troctolite is host to a number of pyroxenitic autoliths ranging in size from a few centimeters to several meters. The autoliths are typically medium- to coarse-grained, dominated by orthopyroxene and with sharp, cuspate contacts. They may display a pronounced enrichment in Cr independent of their visible mineralogy (Fig. 4E, see below). Where visible chromite crystals are absent, chromite can be found as inclusions in silicate phases. ~~This Cr enrichment can also be recognized in PTM's assay intervals comprising troctolite and autoliths (Fig. 13 and 14).~~ The intrusion and emplacement of hot, olivine-phyric silicate liquids into earlier orthopyroxenites is thought to have lead to ~~their~~the therm~~a~~lo-mechanical erosion, transport, and incorporation of orthopyroxenite into younger melt fluxes thereby leading to anomalous Cr contents.

In thin section, the troctolites are characterized by cumulate textured olivine and plagioclase and strong alteration of both minerals. Depending on the sampling location, the sample may contain significant amounts of oikocrystic orthopyroxene and very limited plagioclase (Fig. 5). All major mineral phases may host <50 μm crystals of chromite, often rimmed by magnetite.

Gabbronorites make up the largest part of the TGA Sequence. They form a unit of 100 to 300 m thickness, consisting of varying amounts of orthopyroxene, plagioclase and clinopyroxene. Variations in pyroxene content may bring this unit close to a norite composition, while varying amounts of olivine may occur at the base where the rocks grade into troctolite. This transition usually involves an increase in olivine content with what appears to be a mingling of gabbroic and troctolitic material, often forming discrete areas in core. The unit is generally medium-grained, however rare pegmatoidal patches of gabbroic composition occur. In the southern half of the Waterberg Project the upper TGA Sequence may host a sometimes pegmatoidal, mineralized zone of anorthositic, pyroxenitic, noritic to troctolitic composition (the T Zone). In the study area, these rocks are absent or poorly developed with PGE and Au only weakly elevated (Fig. 14, WB165D0). The controls on the deposition or emplacement of the mineralization are currently unresolved and either non-deposition/emplacement or later erosion appear plausible.

In thin section, the gabbronorites are typical gabbroic cumulate rocks consisting of coarse plagioclase and varying amounts of clino- and orthopyroxene. The latter two may occur as oikocrysts. Upwards through the stratigraphy the amount of clinopyroxene is generally increasing and sporadic inverted pigeonite may be observed. ~~while a~~Alteration throughout the whole sequence is ~~generally limited~~minor. ~~The pyroxenes may occur as oikocrysts. Inverted pigeonite may be observed in this zone, however its occurrence is only sporadic.~~

In other parts of PTM's prospects, the TGA Sequence is overlain by magnetite-bearing gabbros and gabbronorites of the Upper Zone. In the study area, however, these rocks are poorly developed to absent. Due to the fine-grained, disseminated nature of the magnetite in the Upper Zone, the contact can be hard to identify in core and a sharp ~~drop~~rise in magnetic susceptibility due to the appearance of magnetite is taken as the contact.

4.2 Geochemistry

4.2.1 ~~Variation diagrams~~Major and trace element variation diagrams

Data are displayed as bivariate plots with MgO as the differentiation index in Figs. 7 and 8. Variations in major element composition~~s (Table 1)~~ for the rocks analyzed reflect the proportion of

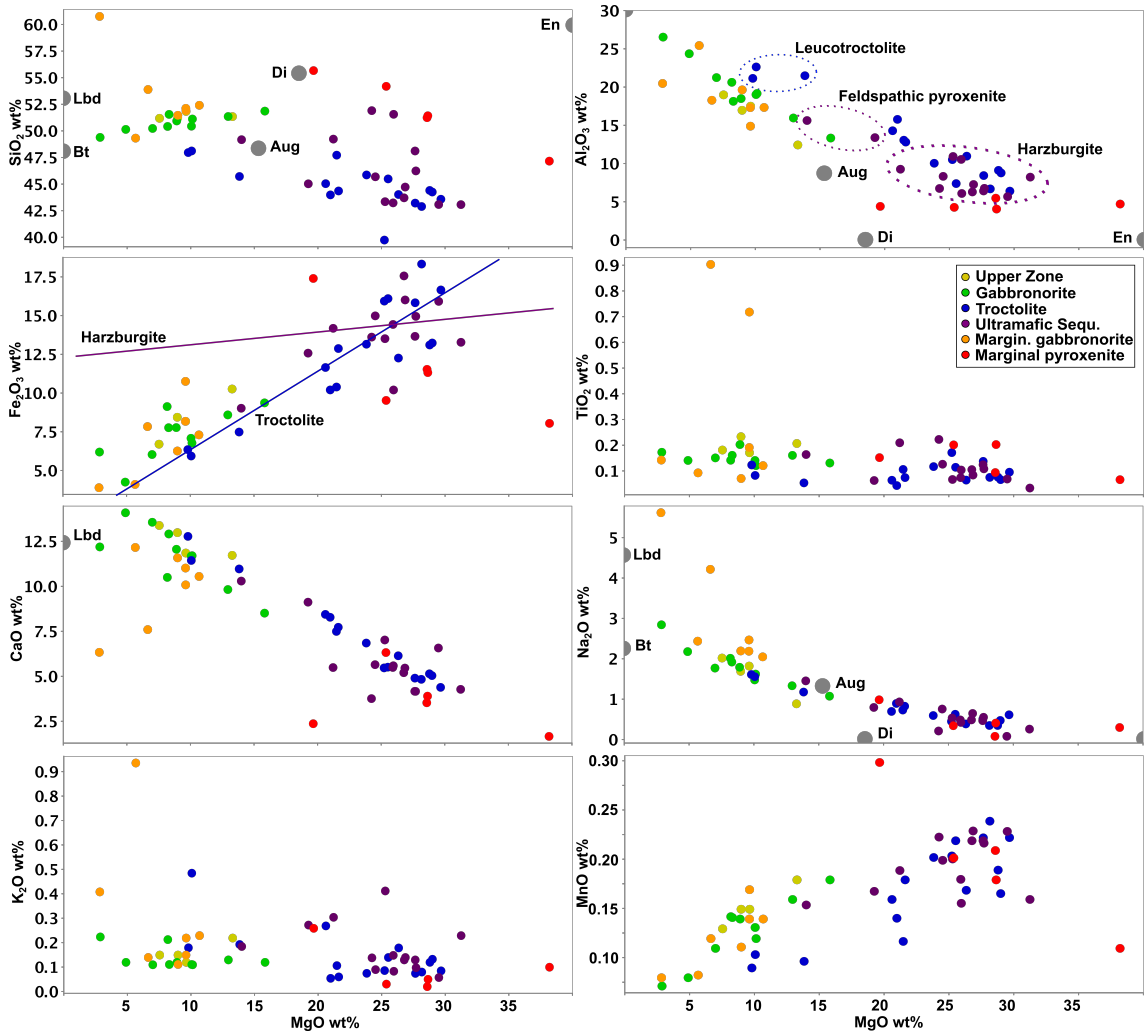

Figure 7: Binary variation diagrams of MgO vs major elements. Except for two samples of feldspathic pyroxenite, the UmS group of samples comprises only harzburgite. The lines in the SiO_2 vs. Fe_2O_3 plot demonstrate the different trends of troctolite and harzburgite (see text). Lbd Labradorite; Bt Bytownite; Aug Augite; Di Diopside; En Enstatite.

olivine, pyroxene and plagioclase present and clearly differentiate between the ~~mostly~~ olivine~~- and~~ + orthopyroxene-dominated Ultramafic Sequence and the plagioclase + clinopyroxene ± olivine ± orthopyroxene ~~and plagioclase~~ assemblages of the TGA Sequence and Upper Zone (Fig. 7; Table 1). ~~Exceptions are three plagioclase-rich (leuco-) troctolite samples which plot towards lower Mg values. Data are displayed as bivariate plots with MgO as the differentiation index in Figs. 7 and 8.~~

~~The rocks have~~ SiO_2 values range~~ing~~ from 40 to 61 wt% ~~with a~~ and decrease towards higher MgO. Three groups of samples can be distinguished: i) harzburgite~~s~~ and 2 feldspathic pyroxenite samples of the UmS form a high-Mg cluster of samples; ii) ~~Marginal~~Basal orthopyroxenites form a separate trend from other samples; iii) rocks of the TGA sequence and UZ, dominated by ~~troctolites and~~ gabbronorite~~s~~ and troctolite, form a trend extending from high- to low-Mg rocks. The wide range of MgO and other major elements for some of the troctolites reflects their cumulus assemblage ranging from ~~dunite~~<90% olivine to leucotroctolite (Fig. 7).

The orthopyroxenites follow a trend of higher SiO_2 for a given MgO than the harzburgites. This elevated SiO_2 reflects the higher SiO_2 in orthopyroxene ~~assemblages~~. Al_2O_3 follows a sharp, de-

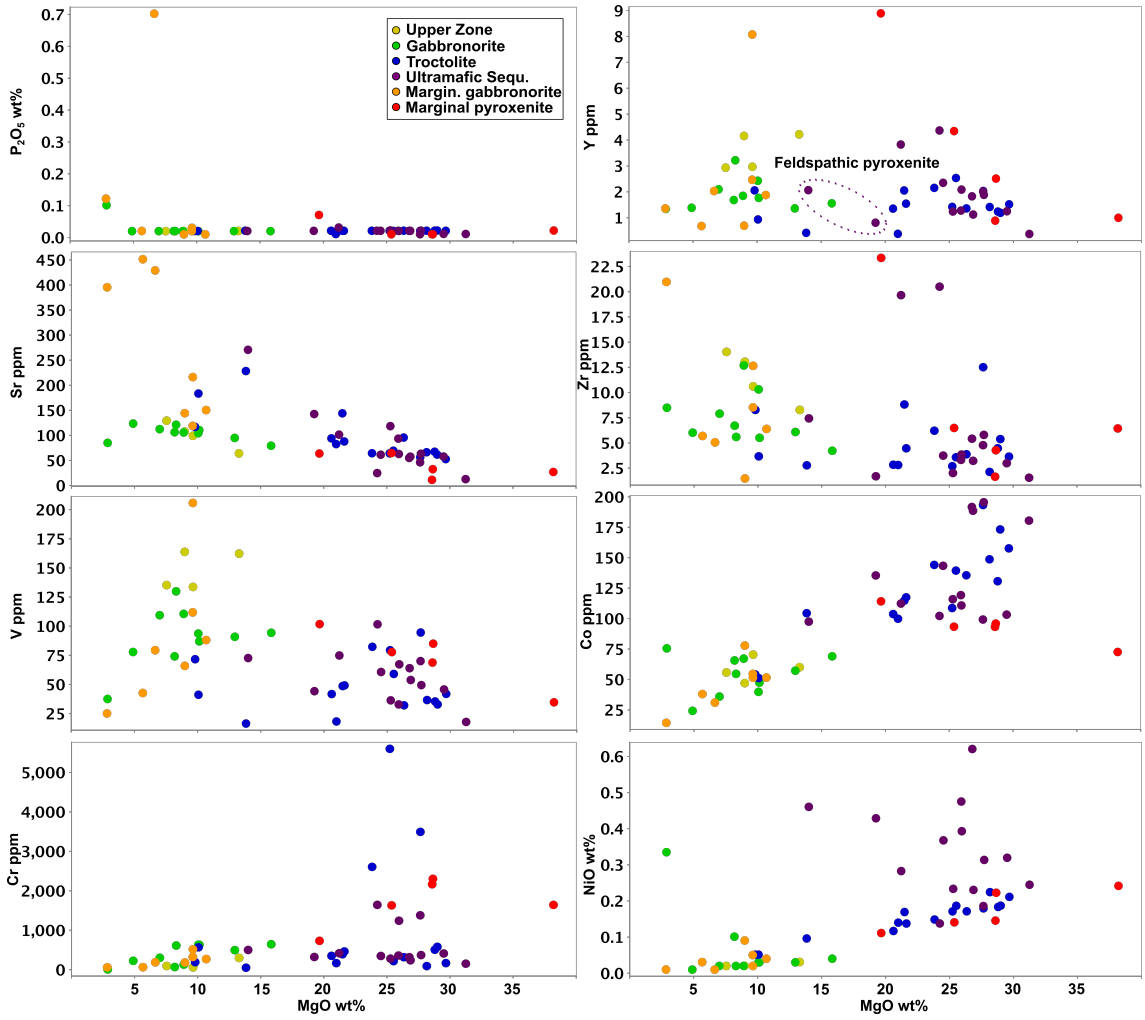

Figure 8: Binary variation diagrams of MgO vs trace elements.

creasing trend with values between 4 and 27 wt%. Fe_2O_3 (as total Fe) decreases with decreasing MgO for most samples, even though there are Mg-rich, orthopyroxenite outliers. Trend lines drawn for the troctolites and harzburgites show that the rocks types follow slightly different trends (Fig. 7). Low Fe_2O_3 values correspond to the paucity of magnetite in the study area. CaO and Na_2O increase with decreasing MgO, reflecting the plagioclase and pyroxene assemblages of the Upper ~~and Main~~ Zone~~s~~ and TGA Sequence. K_2O is generally low with ~~most rocks having~~values between 0.1 and 0.2 wt%. P_2O_5 is less than 0.1 wt% reflecting the absence of apatite even in the Upper Zone. TiO_2 values are low, ~~again~~ corresponding to limited development of the Upper Zone.

~~Gabbronorites and ferrogabbros belonging to the TGA Sequence, Upper Zone and the marginal gabbronorites are characterized by low Fe_2O_3 and elevated Al_2O_3 and Na_2O.~~ V strongly fractionates into magnetite and hence values are higher for Upper Zone samples. NiO is enriched in troctolites, olivine-bearing pyroxenites and due to the presence of sulfides strongly anomalous in mineralized rocks ~~due to the occurrence of sulfides~~. Cr is strongly enriched in ~~samples containing clusters of chromite, i.e. certain~~ pyroxenites and troctolites that contain small chromite clusters. ~~Incompatible~~P_2O_5, Sr and Zr ~~element~~ levels are low in general ~~and their pattern may be influenced by host rock and footwall assimilation for some of the units~~with outliers for the basal gabbronorite (Fig. 8).

4.2.2 Multi-element normalized plots

All samples analyzed show almost identical trends on primitive mantle normalized multi-element plots (Sun and McDonough, 1989). They display negative Th, Nb, Ta and sometimes mildly negative Rb and Ti anomalies while in most cases displaying strong positive Sr and Eu anomalies (Fig. 9). Gabbroic rocks display Rb<Ba, while the opposite is true for the harzburgites and marginal pyroxenites. Mean Rb/Ba_N for the troctolites is 1.

For most groups of samples MREE and HREE are depleted relative to primitive mantle values. Eu/Eu* ranges from 1.1 to 2.1, HREE are generally not fractionated with mean Tb/Yb_N of close to 1. The marginal pyroxenites display significant variation in and have a mean Tb/Yb_N of 1.6 (Fig. 10). LREE are enriched (Mean $Ce/Sm_N = 2$) with mean Ce/Sm_N for the TGA Sequence and basal gabbronorites at 2.7 and 2.2 respectively. Th is enriched relative to Sm, in particular in the troctolites and marginal pyroxenites (Mean $Th/Sm_N = 4.2$ and 3.4, respectively). ~~While~~Although low Eu abundances are expected for the plagioclase-poor pyroxenites, there is some decoupling of plagioclase mode and Eu anomalies.

Samples of UZ, TGA Sequence gabbronorite and troctolites display a tight grouping of ~~analysis~~ results with patterns that are almost identical~~,~~. w~~hereas t~~The marginal pyroxenites, mineralized harzburgites and basal gabbronorites display more within-group variation while still following the overall pattern. Maximum within-group variation is observed in the marginal rocks~~,~~. ~~t~~Their proximity to the granitic footwall may account for some or all of the variation observed, however, some enrichment may also be attributed to trapped liquid (estimated following Maier and Barnes, 1999; McDonald et al., 2009). Regardless of within-sample variation, a small but systematic increase of REE contents can be observed from the troctolites at the base of the succession to the gabbroic units at the top.

4.2.3 PGE and Au

For this study 28 samples from a range of lithologies ~~have been~~were selected for fire assay~~,~~ and the results, normalized to chondrite values (Lodders, 2003), are plotted in Fig. 11. Results for ~~6~~total PGE range from 12 to 12,300 ppb with ~~additional~~ 1.1 to 1100 ppb Au.

Upper Zone and TGA Sequence gabbroic rocks display flat profiles across the IPGE and after a moderate increase of concentration ~~also~~ a flat profile across the PPGE and Au. Samples of the troctolite~~s~~ are mostly characterized by mildly sloping IPGE and except for a mineralized sample ~~by~~have flat PPGE distributions. The ~~S~~serpentinized harzburgit~~eic lithologies~~ exhibits strong~~ly~~ fractionat~~ed~~ion ~~but within this group identical pattern~~ with Pd/Ir of 177. The rocks are enriched in Pd relative to Pt ~~with~~and Au ~~being~~is depleted relative to Pd. This pattern is ~~also seen for the~~identical for that of the mineralized troctolite ~~sample~~. A sample of the basal pyroxenite is characterized by unfractionated PGE (Fig. 11).

Fig. 11 displays variation diagrams of S versus Cu, Pt and Pt. It can be seen that Cu and S exhibit an excellent correlation, whereas the correlation of S and Pt~~/~~ or Pd is significantly ~~weaker~~poorer. Sulfur levels are overall very low with a maximum of c. 12000 ppm. These levels and correlations are identical to commercial assays ~~in the PTM database (see below)~~provided courtesy of Platinum Group Metals.

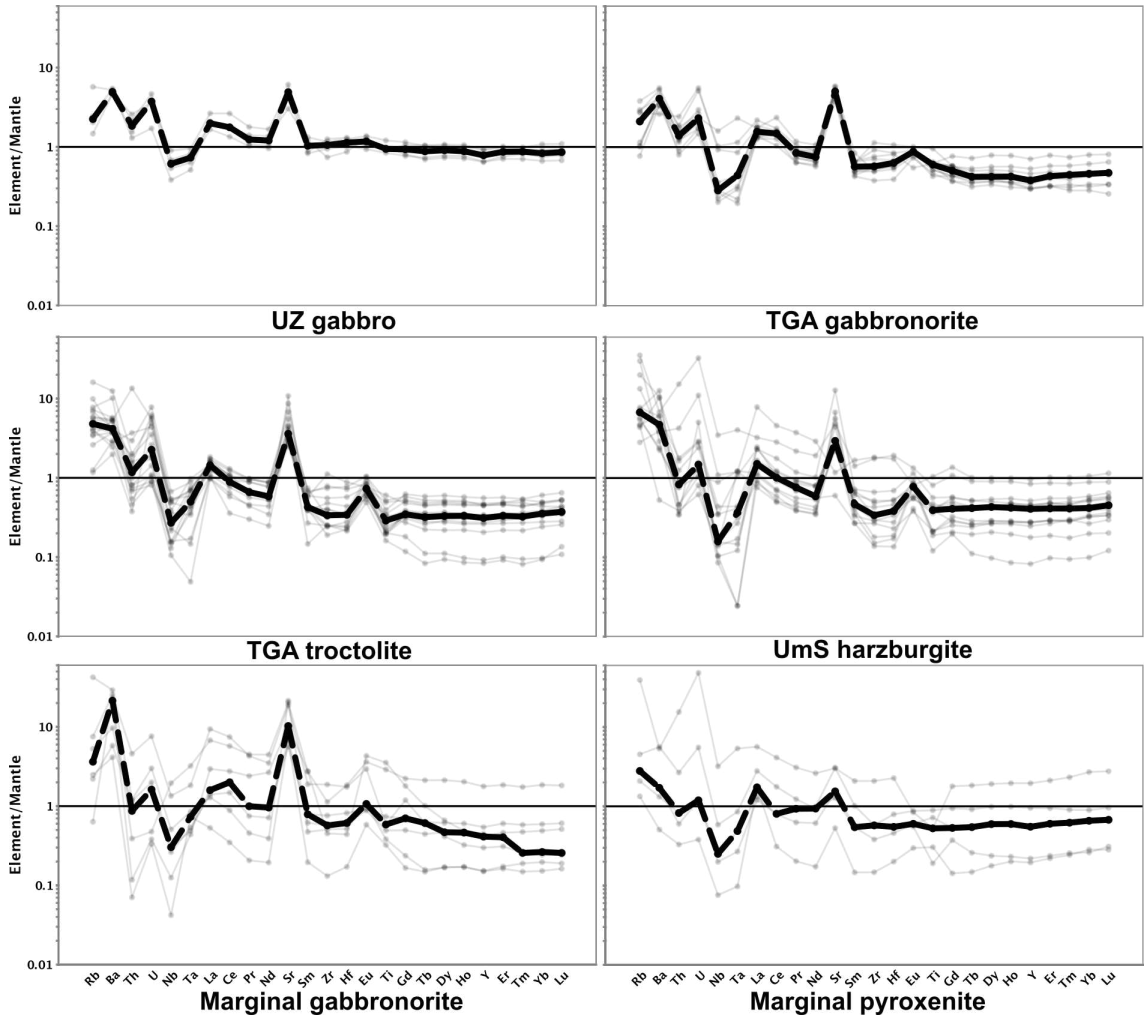

Figure 9: Primitive mantle normalized (Sun and McDonough, 1989) multi-element plots for all six groups of rocks with thick lines showing the average for each group of samples. It can be seen that except for a stratigraphic increase in absolute concentrations the patterns are almost identical. Variations in marginal gabbronorites and pyroxenites are believed to result from contamination by assimilation.

4.2.4 ~~Company assay data~~PGE and Cr assay data provided by Platinum Group Metals

Assay data provided by PTM can be used to assess validity of the results that were presented above. The available assay data for >100 drill holes from the study area was extracted and are~~is~~ shown in the diagrams below.

Figures 12A-C show binary variation diagrams of S vs Cu, Pt and Pd. It can be seen, that Cu and S show excellent correlation whereas there is only a weak correlation of S with~~,~~ Pt and Pd, respectively. Pt and Pd ~~have~~exhibit a good correlation ~~among themselves~~ (Table 2). Figure 12D shows a ternary plot of Pt, Pd and Au. It can be seen, that the majority of assays are dominated by Pd with Pd/Pt approx. 0.6 and only ~~limited~~low Au content. This is in contrast to Pt/Pd observed in the Merensky Reef and closer to the Pt/Pd observed in some sectors of the Platreef (Kinnaird, 2005). Low Au is typical ~~for all~~ of the F Zone, whereas in the T Zone and the Aurora Project Au makes up approximately 20% of the precious metals ~~have approx. 20% Au in the metal~~ budget. Fig. 12D highlights that the anti-correlation of Cr and PGE also applies for the

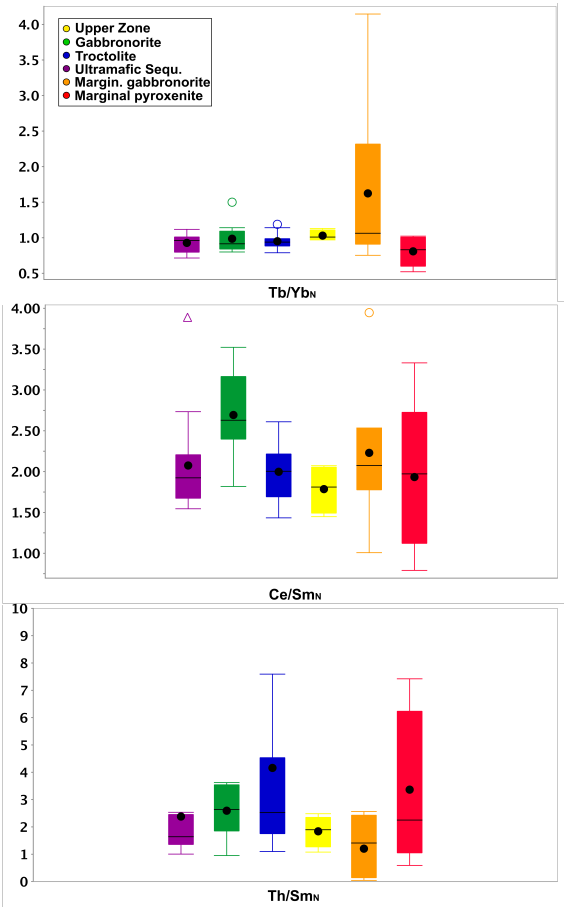

Figure 10: Box plots displaying Tb/Yb_N, Ce/Sm_N and Th/Sm_N values for groups of samples. Color scheme as in Fig. 7. Most variation is exhibited by marginal gabbronorites and pyroxenites, which is interpreted to represent contamination by assimilation. The box represents the inter quartile range with the median represented as horizontal line and the mean as a black circle.

rest of the assays in the area. Is can be seen that a large number of samples plot in between the low-PGE/high-Cr and high-Cr/low-PGE trends. This is due to Cr-rich orthopyroxene autoliths and mingled orthopyroxenitic lithologies that can not be avoided during sampling. This data also experiences a sampling bias towards mineralized samples (the purpose of the company's sampling program) and Cr-rich, unmineralized samples are therefore not well-represented.

4.3 Lateral variation in lithology and mineralization

Typical cross and long sections through the study area (Fig. 3) are shown in Fig. 13 and Fig. 14. Both sections show the dominant lithology and PTM's assay values for 3E (Pt+Pd+Au) and Cr as well as Pt/Pd and Cu/Pd.

Fig. 13 shows a typical sequence of gabbronorite dominated upper TGA Sequence overlying olivine-bearing rocks. The base of the TGA Sequence is characterized by heterogeneous and patchy gabbronorite, norite and troctolite and textures observed in core range from incompletely blended olivine- or pyroxene-dominant patches to discrete autoliths and xenoliths (Fig. 4A, B). Downwards this zone grades into "salt and pepper" textured leuco- to melatroctolite.

Below the troctolite, strongly altered harzburgite hosts the bulk of the mineralization. Orthopyroxenite autoliths occur throughout this part of the succession and where abundant are schematically

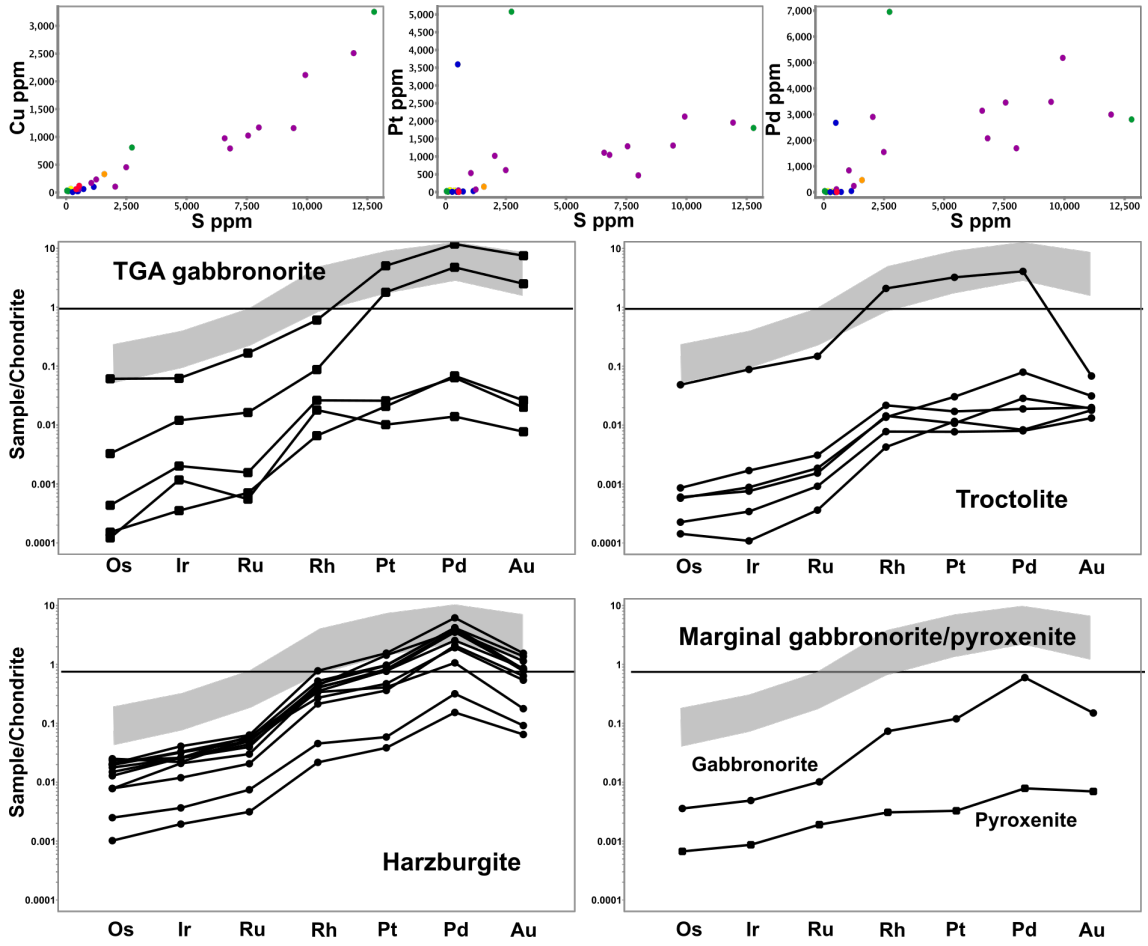

Figure 11: Top: Binary variation diagrams of S vs Cu, Pt and Pd. S vs Cu show an excellent correlation, however the correlation between S and Pt and Pd is weak; Bottom: Chondrite normalized PGE plots for the samples analyzed in this study. Light grey represents PGE distribution from the Turfspruit and Sandsloot high-grade reef-style mineralization in the Northern Lobe (from ~~Yudovskaya et al., submitted~~Yudovskaya et al., 2017).

indicated in the section. These rocks are typically enriched in Cr and their abundance correlates with the Cr concentration. Below the harzburgites may be more orthopyroxenite, basal gabbronorites or more troctolites toward the eastern side of the section (drill hole WB091). The sequence of rocks continues up dip until on the eastern side (not shown) the harzburgites are directly overlain by sedimentary rocks. In zones of mineralization, the Pt/Pd ratio is fairly constant around 0.6 with a Cu/Pd ratio at approximately 530. As shown above, the mineralization is dominated by Pd with little Au in the metal budget.

The four holes in ~~the~~ the long-section (Fig. 14) are located at the western edge of PTMs drilling in this sector (Fig. 3) and mineralization is hosted by strongly altered, ultramafic rocks of varying mineralogy and texture. Holes WB163 and WB049 are located at or around the center of the mineralized zone, while holes WB165 and WB019 are located at its northern and southern edge, respectively. It can be seen that all four holes share a very similar stratigraphy with Cr-enriched intervals that appear to correlate between the holes. Mineralization (shown as Pt+Pd+Au) is most strongly developed in the central section and is poorly developed or absent at the northern and southern sections. The long section shows well-developed troctolite regardless of the thickness and 3E grade of the harzburgite. This suggests that the intrusion of both suites of rocks is independent of each other. Pt/Pd and Cu/Pd are again fairly consistent in the mineralized segments.

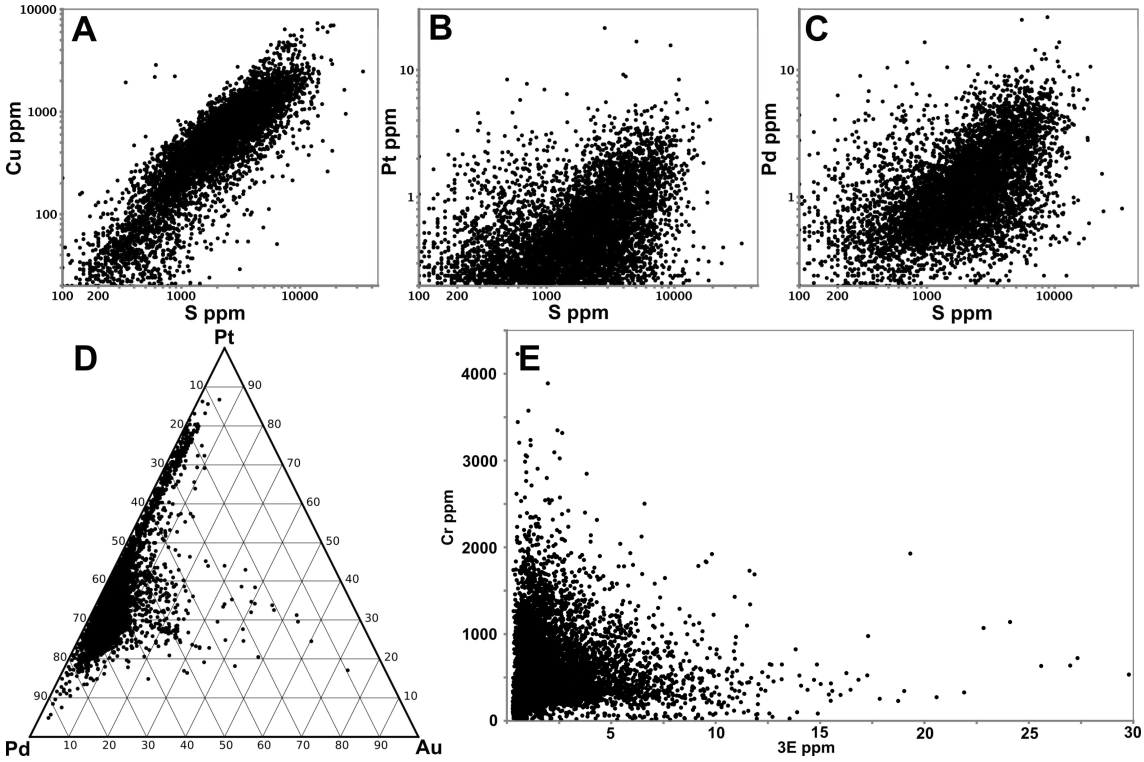

Figure 12: A-C) Binary variation diagrams of chalcophile elements vs sulfur. There is an excellent correlation between Cu and S and a very weak correlation between S and Pt/Pd. D) Ternary diagram showing the relative proportions of Pt, Pd and Au for the assays for the project area. E) Pt+Pd+Au vs Cr diagram highlighting the anti-correlation of precious metals and Cr-rich lithologies. Data filtered for Pt and Pd >0.1 ppm, c. 9500 assays. Sulfide-bearing zones were preferentially sampled by PTM geologists.

In summary, the sections how an SW to NE-oriented, tube-shaped and slightly flattened, mineralized zone of up to 80 m thickness that is dominantly confined to ultramafic rocks. Although most mineralization is confined to harzburgite and feldspathic pyroxenite, in detail the UmS is a highly heterogeneous zone with signs of magma mingling, mixing, fluid flow and sulfide remobilization. Grade ~~i~~drops off towards the northern and southern edges before increasing in the next high-grade, high-thickness harzburgitic zone (not shown in the sections). Grade is also lower in areas of abundant orthopyroxenite and an anti-correlation of Cr and 3E can be seen.

To visualize this area of the Waterberg Project, a Leapfrog 3D model using the logging data from >100 drill holes has been created. Due to the nature of company drill logs, some assumptions and generalizations of logging codes had to be made. This includes grouping various logged rocks into broader categories, but also the assumption that all logged serpentinite is secondary and the product of harzburgite alteration. Additionally, given the nature of the ultramafic rocks, the model uses a >1 g/t 3E grade shell rather than lithology to demonstrate the approximate outline of the UmS. Figure 15A shows the granite-gneiss basement and the up to 80 m thick grade shell. It follows what appears to be a basement depression in a northeasterly direction. To its north, a less-well developed area of PGE mineralization follows the same trend.

These depressions may represent a primary feature controlling magma flow, or alternatively, represent zones of highest heat- and fluid flux and the associated thermal-mechanical erosion. Among researchers associated with this project the tubular intrusions are referred to as chonoliths (e.g Kinnaird et al., 2017). It is important to stress, that this grade shell was not developed by Plat-

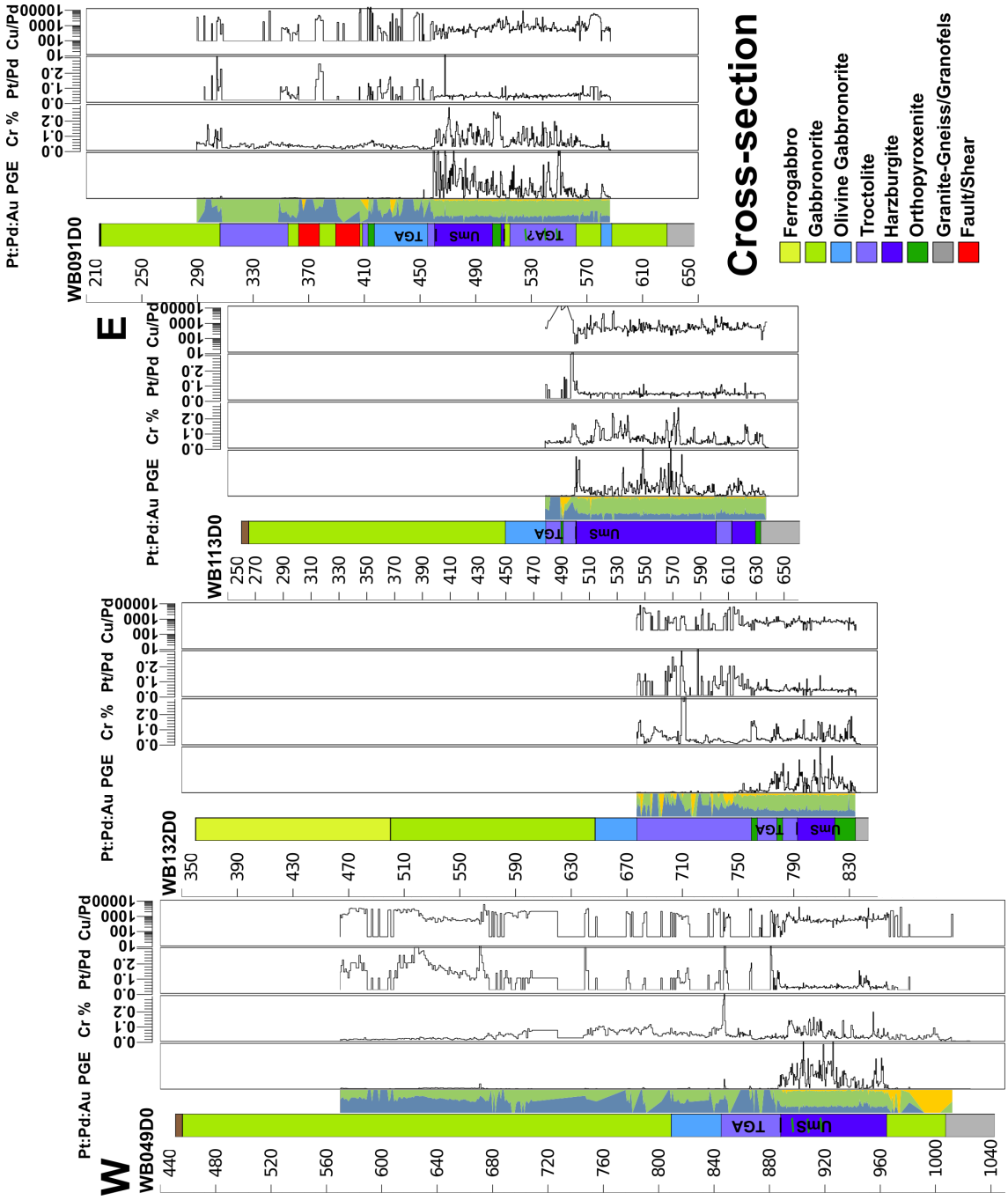

Figure 13: Cross section through the study area as shown in Fig. 3. Columns presented show dominant lithology, the grade of Pt+Pd+Au (no scale), Cr%, Pt/Pd and Cu/Pd extracted from PTM's database. PGE units have been omitted.

inum Group Metals to indicate resources and resources but rather models our understanding of PGE distribution. In Fig. 15B the olivine-bearing lithologies of the lower TGA and Ultramafic Sequence have been added, and the erosional unconformity of the Waterberg Group sediments and dolerite sills are shown. The vertical offset in the dolerite dikes may indicate some fault control. The open area between the upper contact of the olivine-bearing rocks and the base of the sediments is occupied by gabbroic rocks of the TGA Sequence.

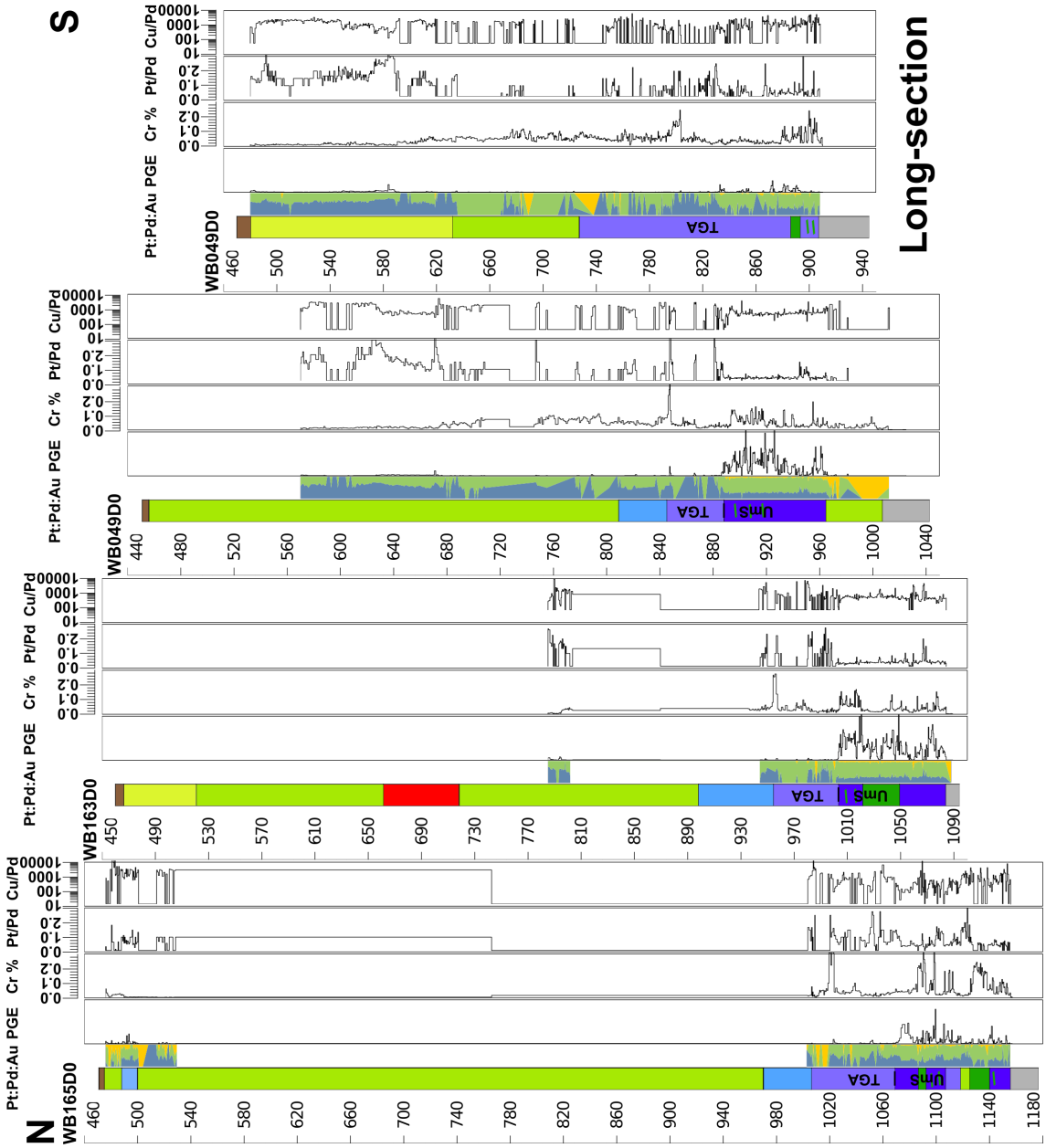

Figure 14: Long section through the study area as shown in Fig. 3. Color scheme as in Fig. 13. Columns presented show dominant lithology, the grade of Pt+Pd+Au (no scale), Cr%, Pt/Pd and Cu/Pd extracted from PTM's database. In contrast to the previous section, harzburgite thickness and associated PGE grade decreases towards the N and S. PGE units have been omitted.

5 Discussion

5.1 Discussion of the data presented

The Northern Lobe of the Bushveld Complex includes the world-class Platreef PGE mineralization and its stratigraphy and mineralization has been the topic of many studies in recent years (e.g. Kinnaird et al., 2005; Kinnaird, 2005; Maier et al., 2008; McDonald and Holwell, 2011; Yudovskaya et al., 2011; Roelofse and Ashwal, 2012; Mitchell and Scoon, 2012; Holwell et al., 2013; Tanner et al., 2014; McDonald et al., 2017; Yudovskaya et al., 2017)~~, also see Yudovskaya et al., subm.)~~.

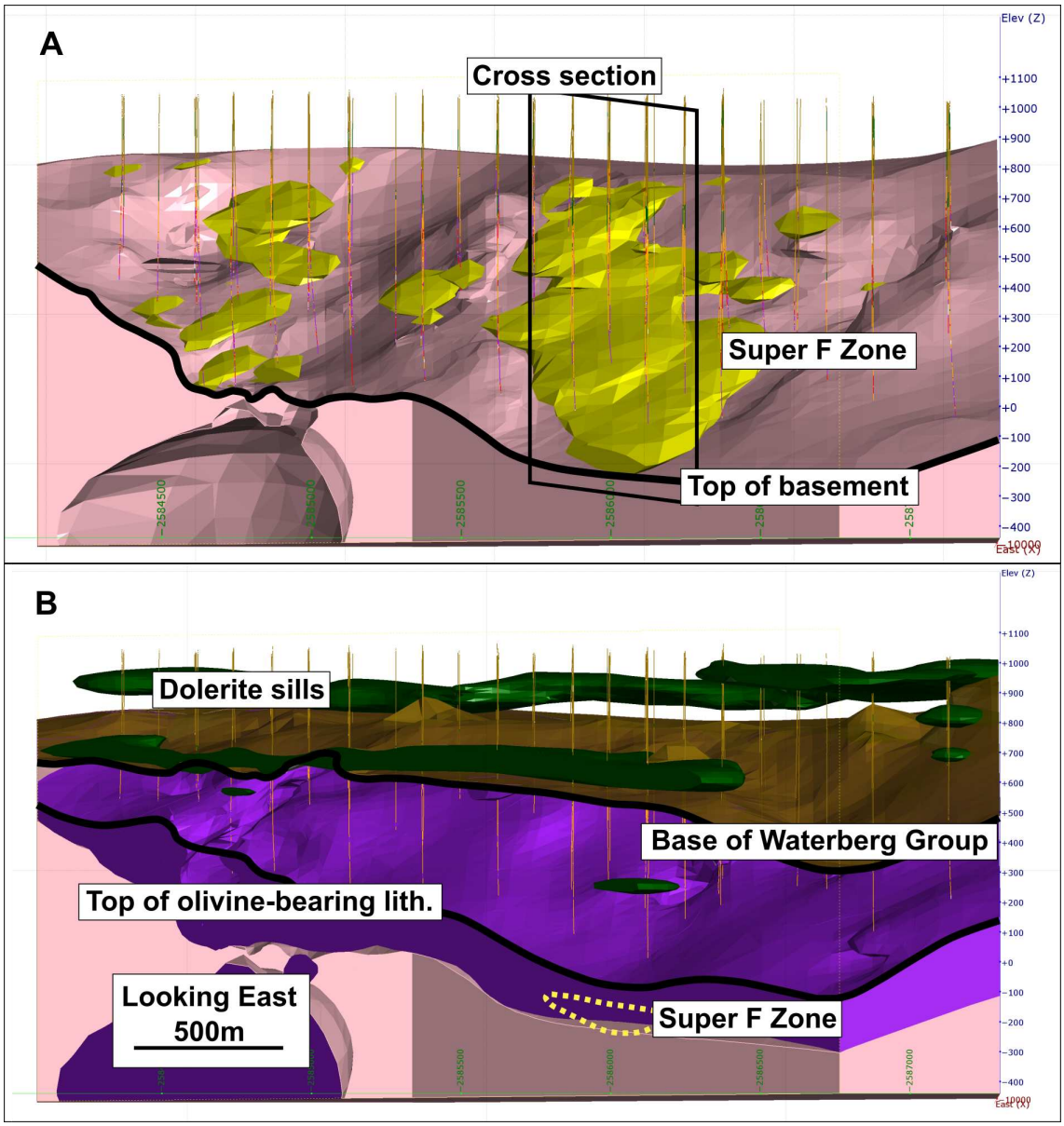

Figure 15: Simplified 3D model of the project area. A) Shown is the geometry of the basement and in yellow a >1 g/t 3E (Pt+Pd+Au) grade shell. The mineralization envelope has a chonolith-shape and is trending in a NE direction. Also shown is the position of holes studied (Fig. 13). B) This panel shows the distribution of the olivine-bearing rocks of the Ultramafic and lower TGA Sequence as logged in PTM's database. The erosional unconformity bringing Waterberg Group sediment in contact with mafic rocks and the dolerite sills are also shown. Note the vertical offset between the two dolerite sheets, perhaps indicating fault control.

In particular ~~T~~the correlation of the Platreef and the Northern Lobe's northernmost, mineralized lithologies at Aurora ~~in particular~~ has recently received some attention (Harmer et al., 2004; Manyeruke, 2007; Maier et al., 2008; McDonald and Harmer, 2010; McDonald et al., 2017). McDonald et al. (2017) describe several key factors that make it unlikely that the Aurora Project is a simple strike extension of the Platreef and instead suggest, that it represents a "marginal facies" of the Main Zone above the Troctolite Marker (which is located 1100 m above the base of the Main Zone). Considering the location of the Waterberg succession less than 20 km north of the Aurora Project, it is appealing to simply link the two zones as a northern magmatic basin. Some of the similarities between the upper Main Zone-hosted Aurora mineralization and the Waterberg T Zone

are provided by McDonald et al. (2017) and this contribution will expand on ~~comments made in~~ their work. ~~As previously mentioned, this contribution has focussed on an area of the Waterberg Succession with little to no development development of the upper mineralized sequence (the T Zone). Nevertheless, both mineralized zones and the whole of the stratigraphy will be considered when discussing possible correlations with the Northern Lobe.~~

In an initial study, laser-ablation U/Pb dating by Huthmann et al. (2016) demonstrated that zircons from mafic rocks of the succession have an age that is within error identical to ages published for the Bushveld Complex. This study also showed, that the sedimentary rocks unconformably overlying the coarse-grained mafic to ultramafic rocks have a maximum depositional age of 2045 Ma with what is interpreted to be an ash-rich paleosoil in-between (Yudovskaya et al., 2015). Given the absence of more evolved mafic rocks, i.e. apatite-bearing UZ or similar, and the absence of any sort of felsic roof rocks, then several kilometers of material must have been removed between c. 2056 and 2045 Ma. The Waterberg Project is characterized by significant erosion, a unique stratigraphy of harzburgites and troctolites, a relatively small size and limited thickness and a position wedged in between the Palala Shear Zone in the North and the Hout River Shear Zone in the South (Fig. 1). This places the succession in a unique situation compared to the rest of the Bushveld Complex. The structural position in particular may have created transtensional spaces and crustal anisotropies along which initial magmas could ascend (Lightfoot and Evans-Lamswood, 2015). Further fault movement until 1.97 Ga brought the succession closer to surface and to a mineable depth (Schaller et al., 1999).

As shown by logging and geochemical data, the samples all represent ultramafic to gabbroic cumulate rocks dominated by varying proportions of olivine, plagioclase, ~~and~~ clino- and orthopyroxene. ~~with c~~Clinopyroxene ~~becoming~~becomes ~~more important~~the dominant pyroxene towards the top of the succession. Pigeonite may be found towards the top of the succession, however its appearance is erratic. The lower part of the succession comprises strongly altered harzburgites and feldspathic pyroxenites hosting the F Zone mineralization and is overlain by troctolites. Contrary what has been described ~~to~~at the nearby Aurora prospect (McDonald et al., 2017), no significant carbonate xenoliths or carbonate alteration has been found in the Waterberg Succession.

The troctolites are different from what is published on the olivine-bearing gabbroic rocks in the Northern Lobe (the Troctolite Marker, van der Merwe, 1976) and comprise only cumulus plagioclase and olivine. The sharp lower contact and the gradational contact with the overlying gabbroic rocks has been shown in drill core (Fig. 4). The Waterberg troctolites are interpreted to be the result of magma mingling and mixing, and are part of a fractionating sequence eroding the earlier harzburgite~~s~~. Consequently, based on available data, they are not believed to be the direct lateral equivalent of the Troctolite Marker in the Northern Lobe, which itself is interpreted to be an influx of primitive magma into a pre-existing Main Zone (Tanner et al., 2014). The PGE-undepleted Troctolite Marker and the cryptic pyroxenite intrusions described by these workers ~~however~~ highlight the significant lateral and vertical variations in the Northern Lobe. Furthermore, although the work of Ashwal et al. (2005) and Roelofse and Ashwal (2012) provides a detailed stratigraphy for most of the Northern Lobe, about 490 m of stratigraphy are unaccounted for. Most crucially, the missing segment is at the base of the troctolite marker where ultramafic rocks might be expected.

Above the olivine-bearing rocks is a package of noritic to gabbronoritic rocks, grading into magnetite-bearing gabbros/gabbronorites. The gabbroic rocks are typically taken to be the equivalent of the Northern Lobe's Main and Upper Zone given their mineralogy. While this may be the case, gabbroic

rocks are typical ~~for~~of evolving layered mafic intrusions and their occurrence does not necessitate a connection of magma conduits between the Northern Lobe and the Waterberg Succession

~~and the occurrence of plagioclase, ortho- and clinopyroxene does not necessitate a connection of magma chambers. The same does apply to magnetite-bearing rocks.~~

The lower part of the succession hosts what are interpreted to be autoliths of Cr-enriched, olivine-bearing orthopyroxenites (which are therefore older). The exact lateral distribution of these rocks is currently ~~insufficiently~~poorly understood, and some may represent either rafts or perhaps simultaneously intruded sills. Where these rocks have been assimilated by younger intrusive phases, the resulting drill core sections are characterized by increased Cr levels (Figs. 13 and 14). Additionally, given their unmineralized nature, a commensurate drop in PGE levels can be observed in the assay intervals including these autoliths (Fig. 13 and 14).~~.~~

Highest PGE grade intervals are often found in zones of intense alteration of primary silicates and may contain sulfide stringers and veins. Both features suggest some remobilization of initial sulfides, also leading to a decoupling of sulfides and to a more limited degree of Pt and Pd. This process can be observed in the company assay data presented earlier, where Pd is remobilized preferentially over Pt (Barnes and Liu, 2012). Whether this process has an effect on the overall Pt/Pd ratio is currently undetermined.

Major element whole-rock geochemistry places the rocks in three distinct groups, representing the Cr-enriched ~~Marginal~~basal ~~O~~orthopyroxenites, the harzburgites of the Ultramafic Sequence, and the Troctolite-Gabbronorite-Anorthosite Sequence and Upper Zone. Rocks of the TGA Sequence form a continuous trend from high-Mg, olivine-rich troctolites to the magnetite-bearing gabbroic rocks ~~higher up in the sequence~~of the Upper Zone. This trend may indicate that the TGA Sequence and the Upper Zone of the Waterberg Succession form a continuum and should be grouped together. The marginal gabbroic rocks resemble the TGA rocks in chemistry and mineralogy, and ~~are thought to be related to~~may represent downward injections into older units~~earlier phases~~. Outliers in troctolite composition may be related to variable amounts of oikocrystic orthopyroxene and contamination by the underlying harzburgite and orthopyroxenite. Trends of harzburgites and troctolites differ, suggesting the crystallization of harzburgite from a more Mg-rich liquid and consequently the crystallization of more Mg-rich olivine.

Normalized REE pattern show near uniformity (e.g. fairly consistent Ce/Yb, Th/Nd) with a minor stratigraphic increase in abundances. Except for Eu, all REE are incompatible in the cumulus phases of the Waterberg succession (olivine, orthopyroxene, plagioclase, clinopyroxene) which is reflected in the primitive mantle-normalized diagrams. Accessory phases (other than zircon) that would concentrate LREE have not been observed and hence the REE budget is controlled by intercumulus liquid (Maier and Barnes, 1998). Normalized REE values below one are interpreted to reflect the fact that the rocks of the Waterberg Succession are crystal cumulates. ~~and that t~~The incompatible element budget of the parental magma was either retained in a staging chamber or lost with migrating interstitial liquid. The variation in incompatible elements and REE contents and the associated extreme outliers, particularly in the basal rocks, are interpreted to represent wall rock contamination. Gabbroic rocks are characterized by $Rb_N < Ba_N$, while the opposite is true for ultramafic rocks. Troctolite Rb/Ba_N are approx. 1, again suggesting contamination of troctolite by underlying harzburgites. Estimates of trapped liquids using La or Zr (not shown; Maier and Barnes, 1999; McDonald et al., 2009) exhibit a good correlation with peaks in incompatible element abundances~~, however~~. ~~g~~Given the interaction of pyroxenites and granite-gneisses observed in drill core, the validity of these calculations, however, is questionable for the Waterberg Succession.

The slight upward stratigraphic increase in LREE observed is interpreted to be related to the increased proportions of clinopyroxene in the rocks. Troughs for the elements Th, Rb, Nb~~,~~ and Ta are fairly typical for Bushveld rocks and generally interpreted to represent contamination by lower-mid continental crust (Barnes and Maier, 2002).

5.2 Correlation with the Aurora Project ~~the Northern Lobe~~

McDonald et al. (2017) recently presented data demonstrating strong similarities between the Aurora Project and parts of the Waterberg Succession. The data presented in their work may be used to create a "simplified" and continuous emplacement model. At this point, most areas of the Northern Lobe are however not nearly as well-researched as the well-exposed open cut mines at Sandsloot. Caution and reliance on published data is therefore needed when correlating individual prospects.

Both the Platreef and the Waterberg Succession exhibit variations in rock type and mineralization along their strike, although compared to the Platreef the Waterberg Succession is small with approximately 15 km strike length. Dynamic emplacement environments with multiple, channelized magma injections along a~~a dip~~westerly to northwesterly direction (rather than a north to south magma flow) have been proposed for the Platreef (Yudovskaya et al., 2017; cf. Barnes et al., 2016), and may together with floor rock control (Kinnaird et al., 2005) be used to explain clear differences along strike. The existing similarities between individual sectors (such as Aurora and the Waterberg Project) may be attributed to the fact, that all of them are related to the Bushveld Large Igneous Province and hence share the same melting event.

McDonald et al. (2017) describe the Aurora Project as consisting of three main units, namely Unit 1 with peridotites and melagabbronorites, Unit 2 with gabbronorites and leucogabbronorites and Unit 3 comprising pigeonite gabbronorites. Additionally, Aurora comprises zones of sometimes pegmatitic magnetite gabbros and olivine-bearing gabbroic rocks. Mineralization is hosted predominantly by felsic rocks. The mineralogical details and geochemical data provided in their work suggests the following correlation:

Unit 1 at Aurora is characterized by orthopyroxenite, enrichment in Cr and consequently high Cr/MgO ratios. These features suggest that Unit 1 might correlate to the Cr-rich marginal orthopyroxenites described for the Waterberg Succession. This interpretation is supported by mineralogy and similar trends and positions on bivariate major and trace element plots and close to identical trace element ratios.

Both Unit 2 and 3 at Aurora are more evolved gabbroic rocks interpreted to correlate with the upper TGA Sequence of the Waterberg Succession. This interpretation is again supported by both mineralogical and geochemical features. Where developed, the upper TGA Sequence in the Waterberg Succession hosts two mineralized zones, often with a middling in between. It features olivine-bearing rocks, the appearance of pegmatites and pigeonite. This is comparable to the variable nature of rocks in the Aurora Project, also characterized by several mineralized zones. Geochemically, available data for the upper TGA Sequence again shares similar positions on bivariate plots and almost identical trace element ratios with the Aurora Project.

The main geochemical difference between the two deposits exists in Rb/Ba_N ratios, with generally lower values for Aurora. McDonald et al. (2017) report a carbonate overprint and carbonate

assimilation for the Aurora project.~~,~~ w~~hile n~~No significant carbonate has been found at the Waterberg, indicating purely granite-gneiss host rocks. The differing Rb/Ba_N ratios ~~are~~may therefore ~~interpreted to~~ be the result of different host rocks.

In terms of previous metals, the Aurora Project is characterized by approximately 20% Au in its precious metals budget (Fig. 16). This also holds true for the T Zone of the Waterberg Project. It is worth noting, however, that elevated Au/PGE ratios have not only been recorded at Aurora, the T Zone and Moorddrift (Harmer et al., 2004; Maier et al., 2008; McDonald and Harmer, 2010; Maier and Barnes, 2010; Holwell et al., 2013; McDonald et al., 2017), but also for the Upper Reef at Turfspruit (Yudovskaya et al., 2017), and the Bastard Reef (albeit at very low levels, Maier and Barnes, 2008). Hence, elevated Au may be a feature associated with higher stratigraphic position in the mafic sequence, given no previous metal depletion. Considering the weak grade at Aurora compared to the Waterberg Project, the prospect might represent a southern extension of the Waterberg Succession rather than the other way around.

This ~~interpreted~~possible correlation between T Zone mineralization and ~~for~~ the Aurora Project does not account for the economically significant F mineralized Zone, which is located stratigraphically below the T Zone. ~~leaves the economically significant lower section of the succession unaccounted for. The F Zone is located stratigraphically below the T Zone and~~ Following the argument of Aurora being located in the upper Main Zone (McDonald et al., 2017), the F Zone ~~may~~must ~~therefore either~~ represent a highly unusual, richly-mineralized lower Main Zone of olivine-bearing rocks, i.e. the Troctolite Marker, or a marginal, very northern expression of the Critical Zone, i.e. the Platreef. ~~Furthermore, i~~

It is crucial to note, that on the farm Harriet's Wish in the far north of the Northern Lobe (Fig. 2A) the igneous units exhibit a pronounced change in strike direction from NNW to NNE when crossing the Hout River Shear Zone. The shear zone itself has, as far as the authors are aware, not been intersected in drill core. Despite the mineralogical and geochemical similarities described above, the exact nature of the relationship of Waterberg Succession and ~~Northern Lobe (s.s.)~~Aurora Project therefore still needs to be established.

5.3 Correlation with the Platreef

Mineralization in the F Zone of the Waterberg Succession is characterized by its anti-correlation with Cr, a Pt/Pd ratio of 0.6 and approximately 5% Au in the metal budget (Fig. 16). Ni/Cu is significantly higher than other Northern Lobe ~~operations~~mines at 6-8. Chondrite-normalized PGE patterns show mildly fractionated IPGE and significantly enriched and also mildly fractionated PPGE. ~~This fractionation between IPGE and PPGE possibly reflects the lower-temperature melts in the Proterozoic (compared to the Archean. Mungall and Brenan, 2014).~~ The PGE have some resemblance to patterns observed at various Platreef projects (Maier et al., 2008 and references therein, ~~Yudovskaya et al., submitted~~Yudovskaya et al., 2017) and what is typical for ultramafic hosts in the Bushveld Complex (Naldrett et al., 2011).~~,~~ ~~although we observe~~The slightly higher fractionation observed between IPGE and PPGE ~~that~~ may be related to IPGE (and chromite) retardation ~~together with chromite~~ somewhere at depth. The low Pt/Pd ratios are typical for those recorded for the lower Platreef (e.g. Kinnaird, 2005) while the (Pt+Pd)/Au and Ni/Cu (adjusted for silicate Ni due to harzburgite host) place the F Zone in a field with Platreef exploration and mining projects (Fig. 4 in McDonald et al., 2017). The absence of a correlation between PGE and S is typical for disseminated mineralization at the base of the Platreef (Hutchinson and Kinnaird, 2005). The poor correlation between the PGE and S is ascribed to the remobilization and partial

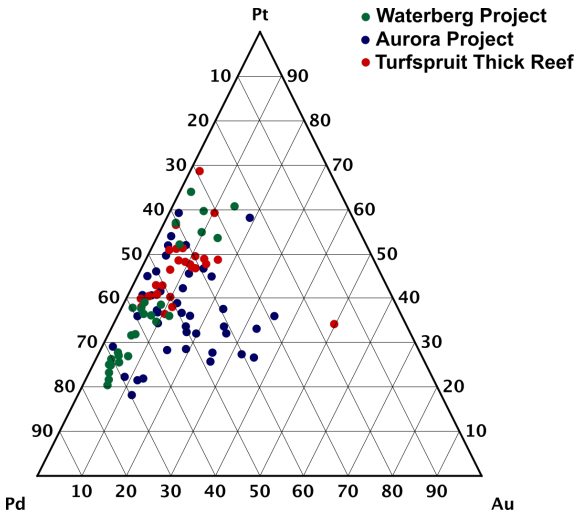

Figure 16: Ternary diagram for Pt, Pd and Au displaying data for the Waterberg Project, the Aurora Project (McDonald et al., 2017) and Turfspruit (Yudovskaya et al., 2017).

removal of sulfides after emplacement, thereby selectively remobilizing Pd over Pt. Cr/MgO ratios are consistently low and dissimilar to the Platreef unit ~~however~~ (McDonald and Holwell, 2011).

Analogously to the Platreef, the mineralized harzburgites and feldspathic pyroxenites are interpreted to have potentially been emplaced as sill- or chonolith-like bodies. Cross- and-long sections as well as a 3D representation of one of the Super F Zones have been presented in Figs. 13, 14 and 15, respectively. In these figures, it can be seen that where the these lithologies are absent, their space it taken up by the otherwise overlying TGA Sequence. This is particularly apparent in Fig. 15, where grade is sparse above the "basement high" in the center of the figure and increases both to the north and south.

The reasons for sulfide saturation are only speculative at present. Possible options may be the assimilation of potentially Cr-rich orthopyroxenites or mixing of successive melt fluxes. Given the granite-gneiss basement and the extreme scarcity of xenoliths ~~of what might have been sedimentary rocks~~, sulfide saturation due to sulfur-rich host-rock assimilations appears unlikely and the sulfur source is under investigation. Detailed petrographic analysis of a wide range of thin sections confirms ~~a~~the remobilization of sulfides observed in core and suspected from geochemical data, and hence the original distribution and mineralogy of the ore minerals is uncertain. Detailed comparisons of the F Zone with the lower part of the troctolite marker are hampered by the lack of published and peer-reviewed descriptions and data.

A preliminary model

In summary, the lower mineralized zone of the Waterberg Project has been shown to have similarities with the Aurora Project and the Platreef, while also displaying clear differences. Any model for the Waterberg Succession must account for the following observations (Kinnaird et al., 2014; Huthmann et al., 2016; Kinnaird et al., 2017):

~~While there is still an abundance of research to be completed, any model for the Waterberg Succession must account for all of the following observations (also see Kinnaird et al., 2014; Huthmann et al., 2016; Kinnaird et al., subm.):~~

- The Waterberg Succession contains a magnetite-bearing gabbroic Upper Zone, a mineralized Troctolite-Gabbronorite-Anorthosite Sequence and a lower, mineralized Ultramafic Sequence of harzburgites and feldspathic pyroxenite.

- The troctolites of the Waterberg Succession are true plagioclase and olivine cumulates unconformably overlying ultramafic rocks. They are characterized by a significant thickness, high-Mg and the fractionation into olivine norite and later gabbronorite.

- The overall thickness of the Waterberg Succession is approximately 25% of the Northern Lobe, however due to an erosional unconformity an unknown amount of material (several km?) as well as roof rocks of unknown nature have as of yet not been intercepted in drill core~~are missing~~.

- The mineralization of the Waterberg T zone contains c. 20% Au in the metal budget. ~~and b~~

- Based on mineralogy and chemistry, the Aurora Project may represent the southern margin of the Waterberg Succession.

- Despite being hosted by harzburgites rather than pyroxenites, the F Zone mineralization shares certain characteristics with the Platreef. It is Pd-dominated and Au-poor, however, Cr/MgO are dissimilar from the Platreef. The Waterberg's F Zone does not form "reefs" and mineralization occurs along high-aspect ratio elongated bodies or chonoliths.

- Geochemical results presented show Bushveld-type cumulate signatures.

Currently many aspects of the development history of the Waterberg Succession are not fully resolved~~, however~~ and its unique structural position ~~may be one major aspect~~is an important example. A simplified model for the evolution of the Waterberg Succession is presented in Fig. 17. The magmatic history of the area is believed to have started with finger-like intrusions~~s~~ of marginal orthopyroxenites intruding into a host rock of granite-gneiss and perhaps overlying sedimentary rocks. Unlike the Northern Lobe, the Waterberg Succession is situated in the Southern Marginal Zone of the Limpopo Belt (van Reenen et al., 1987), wedged in between the Hout River and Palala Shear Zones. Given the tectonic setting of the Limpopo Belt, this initial emplacement may have been facilitated either by pre-existing anisotropies related to faulting or perhaps ongoing faulting during the time of emplacement (Schaller et al., 1999; Clarke et al., 2009; Lightfoot and Evans-Lamswood, 2015). Figure 17 displays the initial stages near a possible basement - cover sequence contact. Whether this is indeed the case is unknown and depth of emplacement may instead be the depth of neutral buoyancy of the ascending ~~liquid~~magma. Given the age and location of the Waterberg Succession (Huthmann et al., 2016), the ~~liquids~~magmas are of course ultimately related to the Bushveld Large Igneous Province.

With increasing magma flux, ~~these~~the magma conduits would experience lateral dilation until eventually forming larger elongated ~~bodies~~lobes. Maximum ~~heat and~~ liquid flux would ~~however~~ be focused on their respective cores, where the crystallization is suppressed due to the high heat flux (Hon et al., 1994). These heated zones of weakness could then be utilized by subsequent intrusion of parental crystal-rich liquids for the harzburgites, in the process widening the conduit while assimilating and transporting earlier rocks (Robertson et al., 2015). The harzburgites are thought to have acted as the transport medium for sulfide droplets, perhaps remobilizing dense sulfide from some initial staging zone (McDonald et al., 2009). Given the tube-like shape of the grade shells and the fairly even distribution of grade throughout the shell, a slumping of sulfides along the basement is not considered viable. ~~Due to recent findings of extremely high partition coefficients~~

~~for PGE (10^5 to 10^6, Mungall and Brenan, 2014), the kinetics of the interaction between sulfide liquid and magma and the architecture of the emplacement zone may however be the crucial factor (Barnes et al., 2016), rather than large pools of sulfide liquid at depth. The geometry of the emplacement zone in particular may be responsible for the substantial thickness and grade of the ore zones, leading to what Platinum Group Metals refers to as Super F Zones.~~Mungall and Brenan (2014) recently demonstrated extremely high partition coefficients of 10^5 to 10^6 for PGE. This means, that the kinetics of the interaction between sulfide liquid and magma and the architecture of the emplacement zone may be more important than large pools of sulfide liquid at depth. The geometry of the emplacement zone in particular may be responsible for the substantial thickness and grade of the Super F Zones. ~~The F Zones and the Waterberg Succession overall are truly exceptional with an indicated resource of more than 24 million ounces 4E the deposit is still open at depth.~~ The position of the mineralized zones and the distribution of sulfides therein again appears to suggest, that the UmS represents zones of crystallization of the respective carrier liquids, and not a basal accumulation of sulfides. Constant Cu/Pd ratios observed in PTMs assay data suggest one common PGE reservoir for this particular Super F Zone. The F Zones and the Waterberg Succession overall are truly exceptional and have an indicated resource of more than 24 million ounces 4E (Pt+Pd+Au+Rh). The deposit is still open at depth.

Following the emplacement of mineralized harzburgitic lithologies, ~~the~~any subsequent intrusion~~s would~~could utilize the extensive pre-heating of country rocks to form a more laterally extensive sheet of troctolites by thermo-mechanical erosion. This was perhaps ~~, perhaps~~ assisted by pre-existing anisotropies along a basement–sedimentary rock interface. At this point, the Waterberg Succession was moving from a stage of finger-like liquid flow and lateral dilation to a stage of sheet-like ~~bodies~~lobes with sufficient thickness to allow for in-situ fractionation. This ultimately led to the formation of a sequence of troctolites–gabbronorites–magnetite-bearing gabbros and to a transition from heterogeneous to homogeneous flow. It is envisioned, that the formation of troctolitic units was related to the mixing of gabbroic and peridotitic crystal-rich ~~liquids~~magmas in the feeder zone of the succession (Renna and Tribuzio, 2011; Saper and Liang, 2014). The subsequent in-situ fractionation of gabbroic magmas may have been disturbed by new cryptic influxes of more gabbroic liquids (cf. Tanner et al., 2014). Fractionation may ~~leading~~have led to ~~a sequence that may have included now eroded fairly evolved rocks of a gabbroic nature~~rocks comparable to what can be seen in the upper Upper Zone of the Northern Lobe (Ashwal et al., 2005), however, in the Waterberg Project this zone has been eroded. ~~Mineralized cores at the base of the troctolites were preserved and the extensive alteration and sulfide remobilization in the harzburgites may be a sign of continuing heat and fluid flux in the system. Occasional pegmatoidal and "vari-textured" rocks throughout the succession perhaps attest to this continuing interaction of heat with the footwall.~~ Mineralized harzburgite "cores" at the base of the troctolites were preserved, and the extensive alteration and sulfide remobilization in the harzburgites may be a sign of continuing heat and fluid flux in the system. The occasional pegmatoidal and "vari-textured" rocks throughout the succession perhaps attest to this continuing interaction of heat with the footwall.

The exact nature of the connection between Waterberg Project and the aforementioned Aurora Project can only be estimated. Taking into account the occurrence of early orthopyroxenites and later gabbroic lithologies, perhaps both areas were connected intermittently with assimilation of dolomite being locally important at Aurora. Correlation of the two projects might indicate that both of them form a northern ~~"basin"~~partially or intermittently connected magmatic basin~~,~~. This basin is internally subdivided by the Hout River and other small shear zones and separated from the south by a basement high south of Aurora (Kinnaird et al., 2005).

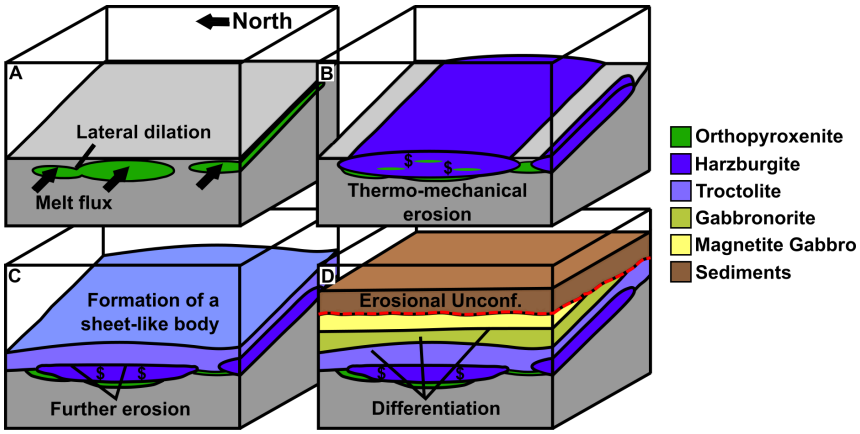

Figure 17: Conceptual model for the emplacement of the lower part (excluding the T Zone mineralization) of the Waterberg Succession. A: Emplacement of marginal orthopyroxenites as finger-like elongated bodies. Lateral dilation with continuing magma flow. B: Emplacement of harzburgitic magma and sulfides by thermo-mechanical erosion of earlier intrusive phases and host rock. C: Emplacement of troctolite~~e~~ic magma, marking the departure from a finger-like geometry and the formation of sheets. D: After the emplacement and fractionation of more magma, the area experienced extensive uplift and the deposition of Waterberg Group Sediments on an erosional unconformity.

As a final step, uplift and later subsidence led to an erosional unconformity and the deposition of Waterberg Group Sediments on top of the succession. This step is crucial, as without significant uplift and erosion the succession might have been covered by ~~what can be assumed to be~~ several kilometers of evolved rocks.

The model presented above requires the intrusion of two distinct magmas during the course of the formation of the Waterberg Succession, one being peridotitic and one gabbroic in character. Given the similarities of the Ultramafic Sequence with the Platreef, and of the TGA Sequence with the Main Zone, it is envisioned that the former crystallized from a Critical Zone-type ~~liquid~~magma while the latter represents a Main Zone-type ~~liquid~~magma (or ~~liquids~~magmas). This is not meant to imply a direct connection of the Waterberg area with either the main Bushveld or the Northern Lobe, but rather refers to the fact that all intrusions belong to the same large igneous province.

6 Conclusion

The Waterberg Succession is a truly outstanding and exciting new PGE discovery, and will change the PGE market with its high grade and thickness ~~change the PGE market~~. It shares ~~common~~ features with mining and exploration prospects to the south, while simultaneously exhibiting unique characteristics. The combination of rock types, type and distribution of mineralization, and tectonic setting is unique and presented here for the first time. Based on observations and geochemical results, the Waterberg Succession may be linked with the Aurora Project to the south, with both projects possibly representing a separate basin rather than a marginal extension of the Northern Lobe. A first conceptual model for the area has been presented and shows how recent advances in our understanding of partition coefficients, fluid dynamics, and the continued work of colleagues in other parts of the Bushveld lead~~s~~ to a better understanding of this magmatic system.

~~The conclusion of the Waterberg Project not representing a mere strike extension of the Northern Lobe is excellent news for explorers of the Bushveld Complex and demonstrates that mineralized~~

~~successions can be found along the margins of the complex. Cooperation of industry and academia, aided by 21st century geophysical techniques may be used to re-evaluate areas previously thought to be barren.~~The conclusion that the Waterberg Succession does not represent a simple strike extension of the Northern Lobe is excellent news for explorers of the Bushveld Complex. It demonstrates, that cooperation of industry and academia, aided by 21st century geophysical techniques, can lead to significant discoveries in well-explored terrains. Rather than obstructing deposit formation, structural features and sedimentary sequences may aid by concentrating melt flow and facilitating later uplift.

Acknowledgements

We would like to acknowledge the support and funding received from Platinum Group Metals. We would also like to acknowledge CIMERA. The work at IGEM RAS was supported by the Russian Foundation for Basic Research (grants 14-05-00448 and 17-05-00456). The manuscript greatly benefited from the detailed comments by P. Lightfoot and W. Maier.

References

Ashwal, L. D., Webb, S. J., Knoper, M. W., 2005. Magmatic stratigraphy in the Bushveld Northern Lobe: continuous geophysical and mineralogical data from the 2950 m Bellevue drillcore. South African Journal of Geology 108 (2), 199–232.

Barnes, S. J., Cruden, A. R., Arndt, N., Saumur, B. M., 2016. The mineral system approach applied to magmatic Ni–Cu–PGE sulphide deposits. Ore Geology Reviews 76 (C), 296–316.

Barnes, S. J., Liu, W., Feb. 2012. Pt and Pd mobility in hydrothermal fluids: Evidence from komatiites and from thermodynamic modelling. Ore Geology Reviews 44 (C), 49–58.

Barnes, S.-J., Maier, W. D., 2002. Platinum-Group Element Distributions in the Rustenburg Layered Suite of the Bushveld Complex, South Africa. In: Cabri, L. J. (Ed.), The Geology, Geochemistry, Mineralogy and Mineral Beneficiation of Platinum-Group Elements. Canadian Institute of Mining, Metallurgy and Petroleum Special Volume 54, pp. 431–458.

Barton, J. M., Klemd, R., Zeh, A., 2006. The Limpopo belt: A result of Archean to Proterozoic, Turkic-type orogenesis? Geological Society of America Special Paper 405, 315–332.

Buick, I. S., Maas, R., Gibson, R. L., 2001. Precise U–Pb titanite age constraints on the emplacement of the Bushveld Complex, South Africa. Journal of the Geological Society 158 (1), 3–6.

Callaghan, C. C., Eriksson, P. G., Snyman, C. P., 1991. The sedimentology of the Waterberg Group in the Transvaal, South Africa: An overview. Journal of African Earth Sciences 13 (1), 121–139.

Cawthorn, R. G., Webb, S. J., 2001. Connectivity between the western and eastern limbs of the Bushveld Complex. Tectonophysics 330 (3-4), 195–209.

Clarke, B., Uken, R., Reinhardt, J., Jul. 2009. Structural and compositional constraints on the emplacement of the Bushveld Complex, South Africa. Lithos 111 (1-2), 21–36.

Corcoran, P. L., Bumby, A. J., Davis, D. W., 2013. The Paleoproterozoic Waterberg Group, South Africa: Provenance and its relation to the timing of the Limpopo orogeny. Precambrian Research 230, 45–60.

Dorland, H. C., Beukes, N. J., Gutzmer, J., Evans, D. A. D., Armstrong, R. A., 2006. Precise SHRIMP U-Pb zircon age constraints on the lower Waterberg and Soutpansberg Groups, South Africa. South African Journal of Geology 109 (1-2), 139–156.

Eales, H. V., Cawthorn, R. G., 1996. The Bushveld Complex. In: Layered Intrusions. Elsevier, pp. 181–229.

Finn, C. A., Bedrosian, P. A., Cole, J. C., Khoza, T. D., Webb, S. J., 2015. Mapping the 3D extent of the Northern Lobe of the Bushveld layered mafic intrusion from geophysical data. Precambrian Research 268, 279–294.

Good, N., de Wit, M. J., Feb. 1997. The Thabazimbi-Murchison Lineament of the Kaapvaal Craton, South Africa: 2700 Ma of episodic deformation. Journal of the Geological Society 154 (1), 93–97.

Grobler, D. F., Nielsen, S. A., Broughton, D., 2012. Upper Critical Zone (Merensky Reef- UG2) correlates within the Platreef on Turspruit Farm, northern limb, Bushveld Complex. In: 6th Platreef Workshop 8th-10th May 2015.

Harmer, R. E., Pillay, N., Davis, P. G., 2004. The Aurora Project - Main Zone hosted PGE-base metal mineralisation at the northern outcrop limit of the Bushveld Northern Limb, north of Mokopane. In: 1st Platreef Workshop, 16-19 July.

Holwell, D. A., Armitage, P. E. B., McDonald, I., Dec. 2005. Observations on the relationship between the Platreef and its hangingwall. Applied Earth Science 114 (4), 199–207.

Holwell, D. A., Jones, A., Smith, J. W., Boyce, A. J., 2013. New mineralogical and isotopic constraints on Main Zone-hosted PGE mineralisation at Moorddrift, northern Bushveld Complex. Mineralium Deposita 48 (6), 675–686.

Holwell, D. A., Jordaan, A., Jun. 2006. Three-dimensional mapping of the Platreef at the Zwartfontein South mine: implications for the timing of magmatic events in the northern limb of the Bushveld Complex, South Africa. Applied Earth Science 115 (2), 41–48.

Holwell, D. A., McDonald, I., Aug. 2006. Petrology, geochemistry and the mechanisms determining the distribution of platinum-group element and base metal sulphide mineralisation in the Platreef at Overysel, northern Bushveld Complex, South Africa. Mineralium Deposita 41 (6), 575–598.

Holzer, L., Frei, R., Barton Jr., J. M., Kramers, J. D., Jan. 1998. Unraveling the record of successive high grade events in the Central Zone of the Limpopo Belt using Pb single phase dating of metamorphic minerals. Precambrian Research 87 (1-2), 87–115.

Hon, K., Kauahikaua, J., Denlinger, R., Mackay, K., 1994. Emplacement and inflation of pahoehoe sheet flows: Observations and measurements of active lava flows on Kilauea Volcano, Hawaii. Geological Society of America Bulletin 106 (3), 351–370.

Huber, H., Koeberl, C., McDonald, I., Reimold, W. U., 2001. Geochemistry and petrology of Witwatersrand and Dwyka diamictites from South Africa: search for an extraterrestrial component. Geochimica et Cosmochimica Acta 65 (12), 2007–2016.

Hulbert, L. J., von Gruenewaldt, G., 1982. Nickel, copper, and platinum mineralization in the lower zone of the Bushveld Complex, south of Potgietersrus. Economic Geology 77 (6), 1296–1306.

Hulbert, L. J., von Gruenewaldt, G., 1985. Textural and compositional features of chromite in the lower and critical zones of the Bushveld Complex south of Potgietersrus. Economic Geology 80 (4), 872–895.

Hutchinson, D., Kinnaird, J. A., 2005. Complex multistage genesis for the Ni–Cu–PGE mineralisation in the southern region of the Platreef, Bushveld Complex, South Africa. Applied Earth Science 114 (4), 208–224.

Huthmann, F. M., Yudovskaya, M. A., Frei, D., Kinnaird, J. A., 2016. Geochronological evidence for an extension of the Northern Lobe of the Bushveld Complex, Limpopo Province, South Africa. Precambrian Research 280, 61–75.

Kinnaird, J. A., Dec. 2005. Geochemical evidence for multiphase emplacement in the southern Platreef. Applied Earth Science 114 (4), 225–242.

Kinnaird, J. A., Hutchinson, D., Schurmann, L., Nex, P. A. M., de Lange, R., 2005. Petrology and mineralisation of the southern Platreef: northern limb of the Bushveld Complex, South Africa. Mineralium Deposita 40 (5), 576–597.

Kinnaird, J. A., Nex, P. A. M., 2015. An Overview of the Platreef. In: Platinum-group element (PGE) mineralisation and resources of the Bushveld Complex, South Africa. An Overview of the Platreef, Council for Geoscience, South Africa, pp. 193–342.

Kinnaird, J. A., Yudovskaya, M. A., Botha, M. J., 2014. The Waterberg Extension to the Bushveld Complex. In: 11th International Platinum Symposium. Yekaterinburg, Russia.

Kinnaird, J. A., Yudovskaya, M. A., McCreesh, M. J. G., Huthmann, F. M., Botha, T. J., 2017. The Waterberg PGE Deposit - atypical mineralization in mafic-ultramafic rocks of the Bushveld Complex, South Africa. Economic Geology 112, 1367–1394.

Kramers, J. D., Mouri, H., 2011. The geochronology of the Limpopo Complex: A controversy solved. In: van Reenen, D. D., Kramers, J. D., McCourt, S., Perchuk, L. L. (Eds.), Origin and Evolution of Precambrian High-grade Gneiss Terranes, with Special Emphasis on the Limpopo Complex of Southern Africa. Geological Society of America Memoir, pp. 85–106.

Kruger, F. J., 2005. Filling the Bushveld Complex magma chamber: lateral expansion, roof and floor interaction, magmatic unconformities, and the formation of giant chromitite, PGE and Ti-V-magnetitite deposits. Mineralium Deposita 40 (5), 451–472.

Lee, C. A., 1996. A review of mineralization in the Bushveld Complex and some other layered intrusions. In: Layered Intrusions. Elsevier, pp. 103–145.

Lightfoot, P. C., Evans-Lamswood, D., 2015. Structural controls on the primary distribution of mafic–ultramafic intrusions containing Ni–Cu–Co–(PGE) sulfide mineralization in the roots of large igneous provinces. Ore Geology Reviews 64 (C), 354–386.

Lodders, K., Jul. 2003. Solar System Abundances and Condensation Temperatures of the Elements. The Astrophysical Journal 591 (2), 1220–1247.

Maier, W. D., Barnes, S.-J., 1998. Concentrations of rare earth elements in silicate rocks of the Lower, Critical and Main Zones of the Bushveld Complex. Chemical Geology 150 (1-2), 85–103.

Maier, W. D., Barnes, S.-J., Nov. 1999. Platinum-Group Elements in Silicate Rocks of the Lower, Critical and Main Zones at Union Section, Western Bushveld Complex. Journal of Petrology 40 (11), 1647–1671.

Maier, W. D., Barnes, S.-J., Sep. 2008. Platinum-group elements in the UG1 and UG2 chromitites, and the Bastard reef, at Impala platinum mine, western Bushveld Complex, South Africa: Evidence for late magmatic cumulate instability and reef constitution. South African Journal of Geology 111 (2-3), 159–176.

Maier, W. D., Barnes, S.-J., 2010. The petrogenesis of platinum-group element reefs in the Upper Main Zone of the Northern Lobe of the Bushveld Complex on the farm Moorddrift, South Africa. Economic Geology.

Maier, W. D., De Klerk, L., Blaine, J., Manyeruke, T., Barnes, S.-J., Stevens, M. V. A., Mavrogenes, J. A., 2008. Petrogenesis of contact-style PGE mineralization in the northern lobe of the Bushveld Complex: comparison of data from the farms Rooipoort, Townlands, Drenthe and Nonnenwerth. Mineralium Deposita 43 (3), 255–280.

Manyeruke, T. D., Mar. 2007. Compositional and lithological variation of the Platreef on the farm Nonnenwerth, northern lobe of the Bushveld Complex: Implications for the origin of Platinum-group elements (PGE) mineralization . Ph.D. thesis, University of Pretoria.

McDonald, I., Harmer, R., Holwell, D. A., Hughes, H. S. R., Boyce, A. J., 2017. Cu-Ni-PGE mineralisation at the Aurora Project and potential for a new PGE province in the Northern Bushveld Main Zone. Ore Geology Reviews 80, 1135–1159.

McDonald, I., Harmer, R. E., 2010. The Nature of PGE mineralization in the Aurora Project Area, Northern Bushveld Complex, South Africa. In: JUGO, P. J., Lesher, C. M., Mungall, J. E. (Eds.), 11th International Platinum Symposium.

McDonald, I., Holwell, D. A., 2011. Geology of the northern Bushveld Complex and the setting and genesis of the Platreef Ni–Cu–PGE deposit. In: Reviews in Economic Geology v. 17. Reviews in Economic Geology, pp. 297–327.

McDonald, I., Holwell, D. A., Armitage, P. E. B., Dec. 2005. Geochemistry and mineralogy of the Platreef and "Critical Zone" of the northern lobe of the Bushveld Complex, South Africa: implications for Bushveld stratigraphy and the development of PGE mineralisation. Mineralium Deposita 40 (5), 526–549.

McDonald, I., Holwell, D. A., Wesley, B., Mar. 2009. Assessing the potential involvement of an early magma staging chamber in the generation of the Platreef Ni–Cu–PGE deposit in the northern limb of the Bushveld Complex: a pilot study of the Lower Zone Complex at Zwartfontein. Applied Earth Science 118 (1), 5–20.

McDonald, I., Viljoen, K. S., 2006. Platinum-group element geochemistry of mantle eclogites: a reconnaissance study of xenoliths from the Orapa kimberlite, Botswana. Applied Earth Science 115 (3), 81–93.

Mitchell, A. A., Scoon, R. N., 2012. The Platreef of the Bushveld Complex, South Africa: Non-sequential Magma Replenishment Based on Observations at the Akanani Project, North-west of Mokopane. South African Journal of Geology 115 (4), 535–550.

Molyneux, T. G., 1974. A geological investigation of the Bushveld Complex in Sekhukhuneland and part of the Steelpoort valley. Transactions of the Geological Society of South Africa, 329–338.

Mungall, J. E., Brenan, J. M., Jan. 2014. Partitioning of platinum-group elements and Au between sulfide liquid and basalt and the origins of mantle-crust fractionation of the chalcophile elements. Geochimica et Cosmochimica Acta 125 (C), 265–289.

Naldrett, A., Kinnaird, J. A., Wilson, A. H., Yudovskaya, M. A., Chunnett, G., 2011. Genesis of the PGE-enriched Merensky Reef and chromitite seams of the Bushveld Complex: . In: Reviews in Economic Geology v. 17. Society of Economic Geologists, pp. 235–296.

Naldrett, A. J., May 2010. Secular Variation of Magmatic Sulfide Deposits and Their Source Magmas. Economic Geology 105 (3), 669–688.

Nicoli, G., Stevens, G., Moyen, J. F., Frei, D., 2015. Rapid evolution from sediment to anatectic granulite in an Archean continental collision zone: the example of the Bandelierkop Formation metapelites, South Marginal Zone, Limpopo Belt, South Africa. Journal of Metamorphic Geology 33 (2), 177–202.

Rajesh, H. M., Santosh, M., Wan, Y., Liu, D., Liu, S. J., Belyanin, G. A., Mar. 2014. Ultrahigh temperature granulites and magnesian charnockites: Evidence for Neoarchean accretion along the northern margin of the Kaapvaal Craton. Precambrian Research 246, 150–159.

Renna, M. R., Tribuzio, R., Aug. 2011. Olivine-rich Troctolites from Ligurian Ophiolites (Italy): Evidence for Impregnation of Replacive Mantle Conduits by MORB-type Melts. Journal of Petrology 52 (9), 1763–1790.

Robertson, J., Ripley, E. M., Barnes, S. J., Li, C., 2015. Sulfur Liberation from Country Rocks and Incorporation in Mafic Magmas. Economic Geology 110 (4), 1111–1123.

Roelofse, F., Ashwal, L. D., 2012. The Lower Main Zone in the Northern Limb of the Bushveld Complex–a >1.3 km Thick Sequence of Intruded and Variably Contaminated Crystal Mushes. Journal of Petrology 53 (7), 1449–1476.

Saper, L., Liang, Y., 2014. Formation of plagioclase-bearing peridotite and plagioclase-bearing wehrlite and gabbro suite through reactive crystallization: an experimental study. Contributions to Mineralogy and Petrology 167:985.

Schaller, M., Steiner, O., Studer, I., Holzer, L., Herwegh, M., Jun. 1999. Exhumation of Limpopo Central Zone granulites and dextral continent-scale transcurrent movement at 2.0 Ga along the Palala Shear Zone, Northern Province, South Africa. Precambrian Research 96, 263–288.

Scoates, J. S., Friedman, R. M., 2008. Precise Age of the Platiniferous Merensky Reef, Bushveld Complex, South Africa, by the U-Pb Zircon Chemical Abrasion ID-TIMS Technique. Economic Geology 103 (3), 465–471.

Scoates, J. S., Wall, C. J., 2015. Geochronology of Layered Intrusions. In: Charlier, B., Namur, O., Latypov, R., Tegner, C. (Eds.), Layered Intrusions. Springer Netherlands, Dordrecht, pp. 3–74.

Seabrook, C. L., Cawthorn, R. G., Kruger, F. J., 2005. The Merensky Reef, Bushveld Complex: mixing of minerals not mixing of magmas. Economic Geology 100, 1191–1206.

Smirnov, A. V., Evans, D. A. D., Ernst, R. E., Söderlund, U., Li, Z.-X., Jan. 2013. Trading partners: Tectonic ancestry of southern Africa and western Australia, in Archean supercratons Vaalbara and Zimgarn. Precambrian Research 224, 11–22.

Smit, C. A., Roering, C., van Reenen, D. D., 1992. The structural framework of the southern margin of the Limpopo Belt, South Africa. In: van Reenen, D. D., Roering, C., Ashwal, L. D., de Wit, M. J. (Eds.), The Archean Limpopo Granulite Belt: Tectonics and Deep Crustal Processes. Precambrian Research, pp. 51–67.

Sun, S. S., McDonough, W. F., 1989. Chemical and isotopic systematics of oceanic basalts: implications for mantle composition and processes. Geological Society, London, Special Publications 42 (1), 313–345.

Tanner, D., Mavrogenes, J. A., Arculus, R. J., Jenner, F. E., 2014. Trace Element Stratigraphy of the Bellevue Core, Northern Bushveld: Multiple Magma Injections Obscured by Diffusive Processes. Journal of Petrology 55 (5), 859–882.

Treloar, P. J., Coward, M. P., Harris, N. B. W., 1992. Himalayan-Tibetan analogies for the evolution of the Zimbabwe Craton and Limpopo Belt. Precambrian Research 55 (1-4), 571–587.

van der Merwe, M. J., 1976. The layered sequence of the Potgietersrus Limb of the Bushveld Complex. Economic Geology 71 (7), 1337–1351.

van Reenen, D. D., Barton, J. M., Roering, C., Smith, C. A., Van Schalkwyk, J. F., 1987. Deep crystal response to continental collision: The Limpopo belt of southern Africa. Geology 15 (1), 11.

von Gruenewaldt, G., Sharpe, M. R., Hatton, C. J., 1985. The Bushveld Complex; introduction and review. Economic Geology 80 (4), 803–812.

Walraven, F., 1997. Geochronology of the Rooiberg Group, Transvaal Supergroup, South Africa. , Information Circular No. 316, Economic Geology Research Unit, University of the Witwatersrand.

Walraven, F., Hattingh, E., 1993. Geochronology of the Nebo Granite, Bushveld Complex. South African Journal of Geology 96 (1/2), 31–41.

Webb, S. J., Cawthorn, R. G., Nguuri, T., James, D., Jun. 2004. Gravity modeling of Bushveld Complex connectivity supported by Southern African Seismic Experiment results. South African Journal of Geology 107 (1-2), 207–218.

Wiebe, R. A., 1980. Commingling of contrasted magmas in the plutonic environment: examples from the Nain anorthositic complex. The Journal of Geology 88 (2), 197–209.

Willemse, J., 1969. The geology of the Bushveld Igneous Complex, the largest repository of magmatic ore deposits in the world. In: Magmatic Ore Deposits - A Symposium. pp. 1–22.

Wilson, A. H., May 2012. A Chill Sequence to the Bushveld Complex: Insight into the First Stage of Emplacement and Implications for the Parental Magmas. Journal of Petrology 53 (6), 1123–1168.

Yudovskaya, M. A., Kinnaird, J. A., Grobler, D. F., Costin, G., Abramova, V. D., Dunnett, T., Barnes, S.-J., 2017. Zonation of Merensky-Style Platinum-Group Element Mineralization in Turfspruit Thick Reef Facies (Northern Limb of the Bushveld Complex). Economic Geology 112.

Yudovskaya, M. A., Kinnaird, J. A., McCreesh, M. J. G., Frei, D., 2015. The lithology at the contact between the Bushveld Mafic–Ultramafic sequence and overlying Waterberg sediments on the Waterberg. In: 6th Platreef Workshop 8th-10th May 2015. pp. 59–61.

Yudovskaya, M. A., Kinnaird, J. A., Naldrett, A. J., Mokhov, A. V., McDonald, I., Reinke, C., 2011. Facies Variation in PGE Mineralization in the Central Platreef of the Bushveld Complex, South Africa. The Canadian Mineralogist 49 (6), 1349–1384.

Yudovskaya, M. A., Kinnaird, J. A., Naldrett, A. J., Rodionov, N., Antonov, A., Simakin, S., Kuzmin, D., 2013a. Trace-element study and age dating of zircon from chromitites of the Bushveld Complex (South Africa). Mineralogy and Petrology 107 (6), 915–942.

Yudovskaya, M. A., Kinnaird, J. A., Sobolev, A. V., Kuzmin, D. V., McDonald, I., Wilson, A. H., 2013b. Petrogenesis of the Lower Zone olivine-rich cumulates beneath the Platreef and their correlation with recognized occurrences in the Bushveld Complex. Economic Geology 108, 1923–1952.

Zeh, A., Ovtcharova, M., Wilson, A. H., Schaltegger, U., 2015. The Bushveld Complex was emplaced and cooled in less than one million years – results of zirconology, and geotectonic implications. Earth and Planetary Science Letters 418, 103–114.

Table 1: Representative geochemical results for rocks analyzed during this study.

Sample ID	UZ1	UZ2	UZ3	UZ4	MZ1	MZ2	MZ3	MZ4	MZ5	MZ6	MZ7	MZ8	MZ9	MZ10	TR1	TR2	TR3	TR4
Rock Type	FEGB	FEGB	FEGB	FEGN	GN	GN	GN	GN	GN	GN	GN	GN	T peg N	T PX	opx TR	peg TR	TR	TR
Group	UZ	UZ	UZ	UZ	MZ	MZ	MZ	MZ	MZ	MZ	MZ	MZ	MZ	MZ	TR	TR	TR	TR
XRF %																		
SiO2	51.34	51.22	51.83	51.18	50.44	51.55	51.35	51.11	51.86	50.14	50.23	50.93	50.42	49.39	43.21	47.72	43.58	44.40
Al2O3	12.43	16.96	17.50	18.98	19.02	18.13	15.96	19.16	13.33	24.36	21.24	18.49	20.62	26.53	8.43	13.05	6.39	9.11
Fe2O3	10.26	8.44	8.17	6.70	7.08	7.76	8.59	6.78	9.37	4.25	6.03	7.77	9.13	6.19	15.83	10.39	16.66	13.10
MnO	0.18	0.15	0.15	0.13	0.13	0.14	0.16	0.12	0.18	0.08	0.11	0.14	0.14	0.07	0.22	0.12	0.22	0.19
MgO	13.28	8.98	9.63	7.55	10.06	8.30	12.94	10.13	15.83	4.89	7.00	8.90	8.18	2.87	27.65	21.48	29.67	28.79
CaO	11.72	12.98	11.85	13.38	11.68	12.91	9.82	11.70	8.51	14.09	13.56	12.06	10.50	12.19	4.90	7.49	4.39	5.14
Na2O	0.88	1.69	1.82	2.02	1.48	1.92	1.33	1.62	1.07	2.18	1.77	1.79	2.01	2.84	0.51	0.73	0.61	0.35
K2O	0.22	0.15	0.12	0.15	0.11	0.11	0.13	0.11	0.12	0.12	0.11	0.12	0.21	0.22	0.07	0.11	0.08	0.12
TiO2	0.21	0.23	0.17	0.18	0.14	0.16	0.16	0.12	0.13	0.14	0.15	0.20	0.14	0.17	0.14	0.11	0.10	0.08
P2O5	0.02	0.02	0.02	0.02	0.02	0.02	0.02	0.02	0.02	0.02	0.02	0.02	0.02	0.10	0.02	0.02	0.02	0.02
Cr2O3	0.06	0.03	0.02	0.02	0.11	0.03	0.12	0.10	0.14	0.05	0.06	0.03	0.01	0.00	0.62	0.10	0.04	0.10
NiO	0.03	0.02	0.02	0.02	0.03	0.02	0.03	0.03	0.04	0.01	0.02	0.02	0.10	0.33	0.18	0.17	0.21	0.18
LOI	3.23	1.38	0.43	0.66	0.46	0.47	0.35	0.47	0.58	0.55	0.47	1.25	1.13	1.48	5.30	5.56	5.39	7.34
Total	99.72	100.12	100.57	99.73	99.66	100.37	99.84	100.38	99.75	99.93	99.75	99.78	100.66	100.34	100.34	100.55	100.49	100.40
S ppm XRF	196	361	NA	172	NA	NA	NA	41	39	95	NA	NA	2731	12786	466	1146	467	269
ICP-MS ppm																		
Li	3.27	2.37	2.06	1.99	2.07	1.35	2.39	3.22	1.03	1.21	2.22	3.19	1.95	2.76	1.45	0.75	3.26	1.56
P	35.08	66.22	40.14	52.69	61.93	21.22	65.47	39.58	33.92	40.68	60.15	71.17	28.60	400.53	63.48	45.03	59.58	31.79
Sc	21.02	17.66	14.57	14.90	12.89	16.35	7.35	10.07	11.76	6.84	9.95	9.09	8.87	1.63	11.04	9.65	7.12	6.56
Ti	1177.14	1567.47	1095.39	1278.42	845.51	811.62	764.64	556.25	605.09	675.87	795.64	1242.24	665.33	804.89	785.45	452.36	402.58	253.98
V	162.31	163.79	133.68	135.28	93.66	129.91	90.92	87.00	94.35	77.85	109.44	110.57	74.13	37.53	94.56	48.63	41.93	35.40
Cr	297.94	162.72	59.75	94.37	632.59	612.41	495.62	632.01	646.01	225.39	301.40	129.36	68.15	7.47	3493.35	391.13	166.84	505.57
Co	60.06	46.99	70.40	55.73	39.81	54.61	57.20	47.39	69.00	24.23	35.94	67.12	65.63	75.55	193.28	114.69	157.70	130.69
Ni	203.37	162.84	175.56	125.56	183.63	501.27	225.06	238.08	228.36	96.46	120.75	163.50	680.41	1949.27	1136.85	1041.82	1372.40	1070.04
Cu	62.70	34.16	69.73	36.97	30.83	48.11	24.37	33.59	26.73	22.48	23.98	33.82	808.77	3251.31	20.63	99.13	37.77	6.64
Zn	59.34	48.73	62.10	49.23	41.63	50.85	52.07	41.69	55.19	24.64	35.76	64.14	55.68	104.01	109.74	50.65	89.92	64.36
Ga	7.69	10.77	13.42	15.01	10.02	12.04	9.60	10.93	7.79	13.53	12.30	13.60	11.42	14.23	7.41	7.64	4.00	4.68
As	0.30	0.36	0.20	0.30	0.31	0.24	0.17	0.21	0.20	0.20	0.21	0.33	0.32	0.26	0.40	0.25	0.18	0.15
Rb	3.64	1.30	0.93	1.55	1.38	0.66	1.88	0.64	1.78	0.49	0.73	1.30	2.42	1.72	2.70	3.75	1.66	3.63
Sr	64.07	107.61	99.20	129.34	104.30	121.14	94.87	110.46	79.34	123.46	112.43	105.81	106.22	85.03	56.33	143.97	52.63	67.33
Y	4.22	4.16	2.97	2.93	2.43	3.22	1.36	1.77	1.56	1.39	2.10	1.85	1.69	1.34	2.03	2.05	1.52	1.24
Zr	8.28	13.05	10.61	14.04	10.31	5.60	6.09	5.51	4.22	6.02	7.90	12.69	6.71	8.49	12.51	8.82	3.64	4.47
Nb	0.27	0.64	0.38	0.49	1.14	0.14	0.26	0.19	0.16	0.20	0.20	0.73	0.20	0.66	0.35	0.26	0.15	0.19
Ba	36.63	32.30	32.55	38.13	26.29	28.24	29.16	28.64	36.80	23.42	23.56	31.40	38.90	18.27	26.24	36.72	26.03	38.80
Sn	0.24	1.14	0.64	3.34	0.41	0.43	0.27	0.38	0.16	0.25	0.32	0.60	0.33	0.54	0.59	0.26	0.19	0.15
Cs	0.17	0.07	0.05	0.05	0.07	0.03	0.06	0.07	0.11	0.02	0.03	0.05	0.21	0.15	0.22	0.45	0.26	0.31
La	1.45	1.82	1.14	1.28	1.19	0.95	1.20	0.87	0.95	0.91	1.28	1.50	0.91	1.20	1.07	1.26	1.01	0.97
Ce	3.09	4.69	2.39	3.19	2.57	2.71	2.50	2.26	1.85	2.48	2.83	3.05	2.81	4.18	1.64	2.31	1.56	1.57
Pr	0.39	0.49	0.28	0.30	0.25	0.25	0.22	0.18	0.18	0.20	0.26	0.29	0.20	0.33	0.25	0.27	0.18	0.17
Nd	1.86	2.26	1.30	1.40	1.12	1.24	0.91	0.81	0.77	0.88	1.15	1.22	0.88	1.44	1.05	1.17	0.81	0.73
Sm	0.53	0.59	0.37	0.39	0.29	0.37	0.20	0.22	0.19	0.22	0.29	0.28	0.22	0.30	0.25	0.29	0.21	0.18
Eu	0.22	0.23	0.16	0.17	0.15	0.16	0.14	0.13	0.12	0.14	0.15	0.17	0.15	0.09	0.13	0.14	0.11	0.11
Gd	0.63	0.68	0.46	0.48	0.34	0.46	0.22	0.26	0.22	0.26	0.34	0.35	0.26	0.34	0.28	0.30	0.23	0.18
Tb	0.11	0.11	0.08	0.08	0.06	0.08	0.03	0.05	0.04	0.04	0.05	0.05	0.04	0.05	0.05	0.05	0.04	0.03
Dy	0.79	0.77	0.57	0.54	0.42	0.58	0.25	0.32	0.27	0.27	0.38	0.35	0.30	0.29	0.34	0.35	0.27	0.21
Ho	0.17	0.16	0.13	0.12	0.09	0.13	0.05	0.07	0.06	0.06	0.08	0.07	0.07	0.06	0.07	0.08	0.06	0.05
Er	0.49	0.47	0.36	0.34	0.28	0.38	0.15	0.21	0.19	0.16	0.23	0.22	0.20	0.15	0.22	0.22	0.17	0.14
Tm	0.07	0.07	0.06	0.05	0.04	0.06	0.02	0.03	0.03	0.03	0.03	0.04	0.03	0.02	0.03	0.03	0.03	0.02
Yb	0.53	0.45	0.37	0.33	0.30	0.39	0.17	0.24	0.22	0.16	0.23	0.22	0.23	0.14	0.23	0.24	0.19	0.16
Lu	0.08	0.07	0.06	0.05	0.05	0.06	0.03	0.04	0.04	0.03	0.04	0.03	0.04	0.02	0.04	0.04	0.03	0.03
Hf	0.27	0.39	0.31	0.41	0.26	0.19	0.17	0.16	0.12	0.17	0.21	0.33	0.20	0.25	0.27	0.22	0.10	0.11
Ta	0.02	0.04	0.03	0.03	0.10	0.01	0.02	0.01	0.01	0.02	0.02	0.05	0.01	0.04	0.03	0.01	0.03	0.03
W	0.03	0.04	0.03	0.03	0.04	0.06	0.03	0.02	0.02	0.03	0.03	0.04	0.02	0.02	0.08	0.02	0.15	0.09
Pb	1.60	0.97	2.05	2.41	0.65	0.95	0.58	0.75	0.62	0.70	0.89	2.08	2.83	14.28	2.68	2.76	1.07	1.71
Th	0.11	0.22	0.13	0.18	0.13	0.07	0.13	0.10	0.11	0.08	0.10	0.16	0.15	0.21	0.16	1.15	0.07	0.08
U	0.04	0.08	0.08	0.10	0.05	0.03	0.06	0.05	0.04	0.04	0.04	0.11	0.06	0.12	0.07	0.12	0.03	0.06
PGE ppb																		
Os	0.29	0.13	NA	0.11	NA	NA	NA	0.07	0.21	0.06	NA	NA	29.7	1.59	0.05	0.23	0.24	0.09
Ir	0.52	0.09	NA	0.10	NA	NA	NA	0.17	0.95	0.55	NA	NA	29.2	5.65	0.04	0.35	0.30	0.13
Ru	0.35	0.21	NA	0.23	NA	NA	NA	0.49	1.08	0.38	NA	NA	115	11.3	0.20	1.11	0.91	0.53
Rh	3.26	0.54	NA	0.53	NA	NA	NA	0.93	3.70	2.53	NA	NA	85.3	12.3	0.53	1.77	1.87	0.99
Pt	20.5	38.7	NA	54.6	NA	NA	NA	20.8	26.0	10.2	NA	NA	5076	1804	10.7	28.8	9.86	7.00
Pd	11.3	20.2	NA	38.6	NA	NA	NA	40.3	37.4	8.20	NA	NA	6951	2805	4.43	45.6	15.8	4.26
Au	2.55	1.46	NA	2.38	NA	NA	NA	3.83	2.90	1.12	NA	NA	1095	365	2.43	4.33	2.61	1.77

Sample ID	TR5	TR6	TR7	TR8	TR9	TR10	TR11	TR12	HZ1	HZ2	HZ3	HZ4	HZ5	HZ6	HZ7	HZ8	HZ9	HZ10
Rock Type	TR	TR	TR	TR	TR	TR	TR	TR	DUN/HZ	HZ- serp	HZ- serp	HZ- serp	HZ- serp	HZ- serp	HZ- serp	HZ- serp	HZ- serp	Serp
Group	TR	TR	TR	TR	TR	TR	TR	TR	HZ	HZ	HZ	HZ	HZ	HZ	HZ	HZ	HZ	HZ
XRF %																		
SiO2	44.02	42.89	45.04	44.35	39.74	45.86	44.25	45.71	44.72	43.71	46.24	48.11	51.56	49.17	49.23	51.90	43.35	45.03
Al2O3	10.97	6.68	14.29	12.81	10.51	10.03	8.77	21.48	7.26	6.28	6.76	6.41	6.08	15.62	9.26	6.74	10.92	13.39
Fe2O3	12.26	18.33	11.65	12.87	15.94	13.15	13.23	7.48	16.01	17.56	14.95	13.66	10.20	9.02	14.18	13.61	13.51	12.58
MnO	0.17	0.24	0.16	0.18	0.20	0.20	0.17	0.10	0.23	0.22	0.22	0.22	0.16	0.15	0.19	0.22	0.20	0.17
MgO	26.34	28.16	20.61	21.62	25.23	23.83	28.99	13.83	26.86	26.77	27.70	27.64	25.95	14.00	21.22	24.24	25.28	19.24
CaO	6.14	4.83	8.44	7.73	5.47	6.85	5.04	10.97	5.46	5.20	4.16	4.17	5.59	10.29	5.49	3.76	7.02	9.12
Na2O	0.39	0.35	0.70	0.83	0.45	0.59	0.47	1.18	0.65	0.49	0.55	0.47	0.42	1.45	0.93	0.21	0.53	0.79
K2O	0.18	0.08	0.27	0.06	0.09	0.07	0.13	0.19	0.14	0.13	0.10	0.13	0.08	0.18	0.30	0.14	0.41	0.27
TiO2	0.06	0.07	0.06	0.07	0.17	0.12	0.07	0.05	0.08	0.11	0.11	0.12	0.10	0.16	0.21	0.22	0.07	0.06
P2O5	0.02	0.02	0.02	0.02	0.02	0.02	0.02	0.02	0.02	0.02	0.02	0.01	0.02	0.02	0.03	0.02	0.02	0.02
Cr2O3	0.06	0.03	0.09	0.08	2.41	0.52	0.13	0.02	0.06	0.08	0.10	0.32	0.28	0.10	0.09	0.30	0.04	0.07
NiO	0.17	0.22	0.12	0.14	0.17	0.15	0.19	0.10	0.23	0.62	0.31	0.19	0.39	0.46	0.28	0.14	0.23	0.43
LOI	6.60	6.46	5.93	5.45	6.47	5.83	9.14	6.47	4.62	4.91	7.51	3.22	3.33	2.26	4.51	5.61	10.13	4.39
Total	99.67	100.24	100.39	99.59	98.95	100.21	100.27	100.44	100.29	99.61	99.86	100.20	99.93	99.81	100.14	100.27	100.36	100.05
S ppm XRF	NA	721	NA	NA	499	NA	NA	NA	NA	11935	2493	1248	6580	9928	8000	525	1044	9442
ICP-MS ppm																		
Li	2.58	2.66	2.22	1.84	2.01	1.92	0.91	7.92	3.28	1.38	2.16	1.37	3.88	5.71	4.72	3.79	4.86	2.18
P	56.53	29.83	24.60	31.13	30.67	13.53	30.21	20.90	26.87	62.32	50.58	32.88	21.54	46.99	83.19	59.74	20.43	15.59
Sc	7.62	7.93	8.62	10.77	9.44	13.00	7.03	1.70	9.00	9.43	11.46	12.85	15.44	9.35	15.38	19.11	7.53	7.63
Ti	269.05	252.65	284.68	346.79	437.16	638.26	310.53	262.86	513.37	535.98	557.96	612.95	467.20	733.83	1051.95	1352.20	274.05	245.32
V	32.09	36.62	41.77	49.20	79.38	82.32	32.86	16.44	53.82	63.97	49.45	70.05	67.29	72.66	74.88	101.64	36.37	44.24
Cr	316.68	91.64	351.49	462.63	5598.44	2606.25	580.25	50.59	238.54	318.08	370.93	1378.88	1241.13	500.13	416.92	1643.24	280.91	322.41
Co	135.57	148.71	103.73	117.47	108.67	144.09	173.25	104.44	188.62	191.68	195.57	99.23	110.82	97.48	112.33	102.20	115.95	135.46
Ni	1023.52	1271.49	630.69	862.13	928.64	878.10	1052.88	661.21	1495.61	4062.16	1819.59	930.41	2498.85	2963.47	1839.36	796.96	1282.99	2616.62
Cu	10.68	60.70	45.65	44.66	23.45	39.55	7.11	49.81	184.85	2507.57	453.47	233.49	975.01	2114.10	1169.29	61.51	171.33	1157.92
Zn	66.08	109.24	61.50	62.54	63.46	95.41	86.37	50.99	115.65	102.36	96.91	61.12	69.04	48.77	75.61	113.88	81.89	61.30
Ga	5.86	4.02	6.87	6.87	5.53	8.04	5.58	10.08	5.49	3.82	5.77	4.10	4.09	8.22	7.22	7.63	5.20	6.39
As	0.19	0.17	0.21	0.21	0.16	0.28	0.35	0.32	0.35	0.17	0.32	0.18	0.32	0.36	0.30	1.47	0.69	0.18
Rb	4.59	2.17	4.32	0.80	2.52	2.50	6.29	4.93	4.41	2.78	4.92	3.64	3.46	3.00	22.50	8.50	12.68	4.68
Sr	95.63	66.29	93.99	87.83	64.01	64.30	61.58	228.31	57.50	54.94	63.24	46.20	62.86	270.68	101.47	24.73	118.38	142.52
Y	1.36	1.42	1.35	1.55	1.42	2.15	1.19	0.42	1.13	1.83	1.88	2.01	2.09	2.07	3.83	4.37	1.24	0.81
Zr	3.87	2.12	2.84	4.47	2.69	6.21	5.38	2.78	3.23	5.42	5.80	4.78	3.85	7.44	19.66	20.51	2.01	1.69
Nb	0.19	0.08	0.09	0.11	0.17	0.37	0.48	0.11	0.12	0.25	0.25	0.63	0.11	0.31	2.48	0.78	0.06	0.08
Ba	40.18	26.07	29.81	20.53	17.14	19.52	28.40	70.94	30.68	71.48	41.79	15.78	16.76	42.56	47.46	26.52	73.90	88.55
Sn	0.22	0.17	0.18	0.21	0.23	0.45	0.25	0.22	0.41	0.81	0.72	0.26	0.44	0.68	0.59	0.55	1.05	0.59
Cs	0.68	0.31	0.31	0.02	0.26	0.09	0.66	0.27	0.25	0.57	1.17	0.32	0.52	0.20	1.76	0.97	2.01	0.49
La	1.08	0.67	0.89	0.85	0.76	1.10	0.91	0.68	0.64	1.15	1.59	0.79	0.92	1.60	2.23	5.40	0.73	0.59
Ce	1.68	1.03	1.49	1.59	1.35	1.85	1.47	1.15	0.91	2.10	2.18	1.27	1.75	3.14	5.06	8.13	1.23	1.04
Pr	0.19	0.13	0.17	0.19	0.16	0.25	0.19	0.12	0.12	0.25	0.26	0.15	0.20	0.33	0.60	1.03	0.14	0.11
Nd	0.81	0.59	0.74	0.81	0.70	1.03	0.78	0.47	0.53	1.08	1.09	0.72	0.82	1.39	2.59	3.93	0.58	0.47
Sm	0.19	0.18	0.19	0.19	0.17	0.26	0.17	0.12	0.15	0.30	0.27	0.20	0.21	0.32	0.63	0.74	0.18	0.16
Eu	0.11	0.10	0.14	0.14	0.10	0.13	0.09	0.12	0.09	0.13	0.14	0.10	0.09	0.19	0.23	0.14	0.14	0.13
Gd	0.21	0.21	0.20	0.22	0.20	0.31	0.19	0.11	0.17	0.28	0.30	0.24	0.25	0.34	0.64	0.82	0.18	0.12
Tb	0.03	0.03	0.04	0.04	0.03	0.05	0.03	0.01	0.03	0.05	0.05	0.04	0.05	0.06	0.10	0.11	0.03	0.02
Dy	0.23	0.25	0.24	0.26	0.24	0.37	0.20	0.08	0.20	0.33	0.32	0.32	0.32	0.37	0.67	0.74	0.21	0.15
Ho	0.05	0.06	0.05	0.06	0.05	0.08	0.04	0.02	0.04	0.07	0.07	0.08	0.08	0.08	0.15	0.16	0.05	0.03
Er	0.15	0.16	0.16	0.17	0.16	0.23	0.13	0.05	0.13	0.19	0.21	0.23	0.23	0.23	0.42	0.49	0.14	0.09
Tm	0.02	0.02	0.02	0.03	0.02	0.04	0.02	0.01	0.02	0.03	0.03	0.04	0.03	0.03	0.06	0.08	0.02	0.01
Yb	0.17	0.18	0.16	0.18	0.17	0.25	0.14	0.05	0.13	0.19	0.22	0.25	0.27	0.25	0.44	0.52	0.16	0.10
Lu	0.03	0.03	0.03	0.03	0.03	0.04	0.02	0.01	0.02	0.03	0.04	0.04	0.04	0.04	0.07	0.09	0.03	0.02
Hf	0.10	0.07	0.08	0.11	0.09	0.18	0.14	0.07	0.10	0.16	0.16	0.14	0.12	0.21	0.60	0.54	0.06	0.05
Ta	0.02	0.00	0.02	0.02	0.01	0.03	0.04	0.01	0.01	0.02	0.04	0.05	0.01	0.02	0.17	0.05	0.00	0.00
W	0.07	0.11	0.02	0.03	0.00	0.03	0.09	0.01	0.11	0.41	0.12	0.02	0.08	0.07	0.18	0.21	0.10	0.08
Pb	0.67	1.59	0.39	0.38	0.92	1.07	2.34	1.13	5.50	9.92	9.67	0.85	2.00	2.67	5.18	1.83	1.02	5.46
Th	0.14	0.04	0.12	0.06	0.06	0.31	0.25	0.05	0.04	0.14	0.11	0.07	0.07	0.15	1.30	0.36	0.04	0.03
U	0.04	0.02	0.04	0.02	0.02	0.09	0.16	0.02	0.03	0.06	0.05	0.02	0.03	0.06	0.69	0.23	0.02	0.02
PGE ppb																		
Os	NA	0.35	NA	NA	22.6	NA	NA	NA	NA	11.2	14.44	1.33	4.32	11.8	4.35	0.53	13.51	11.38
Ir	NA	0.68	NA	NA	40.7	NA	NA	NA	NA	18.0	12.16	1.92	11.6	23.1	6.48	1.00	14.49	18.50
Ru	NA	1.87	NA	NA	102	NA	NA	NA	NA	41.5	45.89	5.87	24.8	53.5	16.8	2.41	50.91	47.81
Rh	NA	2.86	NA	NA	322	NA	NA	NA	NA	81.2	49.12	7.73	73.3	146	38.4	3.61	61.86	96.51
Pt	NA	15.9	NA	NA	3594	NA	NA	NA	NA	1955	617.74	71.7	1108	2125	470	46.34	534.64	1309.31
Pd	NA	10.33	NA	NA	2675	NA	NA	NA	NA	2993	1548.93	241	3141	5178	1695	113.25	840.29	3482.22
Au	NA	2.71	NA	NA	9.69	NA	NA	NA	NA	224	103.58	16.6	150	307	123	11.55	32.77	162.53

Sample ID	HZ11	HZ12	BGN!	BGN!	BGN!	BGN!	BGN!	BGN!	BGN!	BPX1	BPX2	BPX3	BPX4	BPX5
Rock Type	Serp	HZ	AN/basal N	basal GN	AN	basal GN	basal GN	GN	px AN (LN)	chr PX	ol (fsp) PX	ol OPX	ol OPX	OPX
Group	HZ	HZ	basal GN	basal GN	basal GN	basal GN	basal GN	basal GN	basal GN	basal PX	basal PX	basal PX	basal PX	basal PX
XRF %														
SiO2	43.08	45.69	60.76	49.32	53.89	51.92	51.46	52.41	52.12	51.24	55.67	51.42	47.16	54.19
Al2O3	5.67	8.32	20.47	25.43	18.27	14.88	19.63	17.33	17.31	5.47	4.39	4.05	4.70	4.27
Fe2O3	15.92	14.98	3.89	4.10	7.84	10.75	6.26	7.30	8.17	11.53	17.40	11.32	8.04	9.52
MnO	0.23	0.20	0.08	0.08	0.12	0.17	0.11	0.14	0.14	0.21	0.30	0.18	0.11	0.20
MgO	29.50	24.52	2.83	5.66	6.64	9.62	8.99	10.68	9.61	28.58	19.66	28.64	38.20	25.37
CaO	6.57	5.65	6.33	12.16	7.60	10.08	11.58	10.55	11.02	3.53	2.37	3.90	1.66	6.32
Na2O	0.08	0.76	5.62	2.44	4.22	2.47	2.19	2.05	2.19	0.08	0.98	0.41	0.30	0.34
K2O	0.06	0.09	0.41	0.94	0.14	0.22	0.11	0.23	0.15	0.02	0.26	0.05	0.10	0.03
TiO2	0.07	0.13	0.14	0.09	0.90	0.72	0.07	0.12	0.19	0.09	0.15	0.20	0.07	0.20
P2O5	0.01	0.02	0.12	0.02	0.70	0.03	0.01	0.01	0.02	0.01	0.07	0.01	0.02	0.01
Cr2O3	0.09	0.07	0.02	0.02	0.04	0.08	0.04	0.05	0.06	0.46	0.12	0.50	0.43	0.34
NiO	0.32	0.37	0.01	0.03	0.01	0.02	0.09	0.04	0.05	0.15	0.11	0.22	0.24	0.14
LOI	12.39	4.80	1.54	2.71	0.34	1.09	0.63	0.56	0.55	3.91	1.12	1.24	9.04	0.64
Total	100.16	99.43	100.33	99.91	99.67	100.00	99.99	100.25	100.29	100.34	99.89	99.88	100.30	100.06
S ppm XRF	2036	6805	NA	NA	NA	NA	1586	NA	NA	NA	NA	NA	415	542
ICP-MS ppm														
Li	1.96	0.90	9.98	17.18	3.11	7.37	2.61	7.87	5.07	3.41	1.95	0.54	0.68	1.22
P	21.40	26.38	494.88	49.42	3053.13	88.84	5.92	20.86	40.51	15.24	279.71	20.74	46.31	38.77
Sc	9.82	12.24	2.70	3.77	4.87	20.58	7.49	13.81	12.54	12.22	27.21	12.50	5.36	16.09
Ti	279.65	508.05	761.40	497.20	4600.15	3763.27	419.44	640.96	958.40	397.05	685.38	936.37	247.78	1158.50
V	45.69	60.69	25.11	42.69	79.39	205.75	65.96	88.08	111.84	68.77	101.80	85.02	34.68	77.78
Cr	411.38	348.05	58.49	63.82	188.22	516.51	181.96	269.96	322.48	2165.51	731.82	2302.85	1642.61	1631.25
Co	103.26	143.36	14.35	38.02	30.98	51.46	77.81	51.54	54.52	93.25	114.16	95.92	72.57	93.35
Ni	1451.10	2112.82	36.09	197.21	70.01	172.12	620.61	271.44	297.95	763.23	618.28	1205.41	1326.61	916.00
Cu	103.80	791.92	9.91	22.30	24.73	53.06	329.66	58.76	256.35	65.67	250.92	695.22	58.77	119.74
Zn	46.68	75.12	47.29	36.38	71.48	88.32	47.96	46.24	50.90	64.50	162.81	70.08	32.78	115.86
Ga	2.65	5.75	19.47	16.38	15.54	14.57	14.31	11.10	11.13	3.04	7.54	3.51	2.80	4.67
As	1.11	0.19	0.17	0.34	0.23	0.46	0.30	0.22	0.20	0.17	0.53	0.13	0.25	0.24
Rb	2.92	1.79	4.79	26.87	0.40	2.31	1.58	3.36	1.40	0.85	24.92	1.32	2.88	1.77
Sr	57.72	61.39	395.40	451.43	429.09	216.27	144.25	150.52	118.98	11.23	63.75	32.54	26.95	64.63
Y	1.25	2.35	1.36	0.68	2.03	8.07	0.69	1.88	2.47	0.89	8.89	2.51	1.00	4.35
Zr	2.99	3.74	20.98	5.69	5.06	12.65	1.47	6.39	8.52	1.65	23.36	4.27	6.44	6.49
Nb	0.10	0.11	0.96	0.36	1.39	0.09	0.03	0.19	0.22	0.05	2.28	0.18	0.42	0.14
Ba	3.68	27.37	177.67	203.28	159.87	149.39	28.91	67.69	40.58	3.55	37.22	9.24	39.30	11.96
Sn	0.43	0.39	0.39	0.31	0.21	0.91	0.32	2.49	0.39	0.42	0.73	0.55	0.32	1.18
Cs	0.86	0.28	0.36	0.63	0.03	0.31	0.11	0.14	0.09	0.36	2.55	0.09	0.45	0.28
La	0.52	1.10	6.45	0.88	4.65	2.03	0.37	0.96	1.09	1.19	3.88	0.90	1.92	0.82
Ce	0.88	1.93	13.24	1.57	10.15	4.89	0.62	2.63	3.55	0.55	7.31	1.41	3.13	1.43
Pr	0.11	0.24	1.19	0.13	1.24	0.66	0.06	0.21	0.28	0.06	0.85	0.17	0.34	0.26
Nd	0.49	1.05	4.73	0.53	6.03	3.60	0.26	0.97	1.30	0.23	3.54	0.83	1.27	1.34
Sm	0.12	0.29	0.84	0.21	1.22	1.22	0.09	0.27	0.35	0.07	0.93	0.24	0.24	0.45
Eu	0.06	0.16	0.50	0.18	0.72	0.61	0.10	0.15	0.16	0.05	0.14	0.10	0.09	0.15
Gd	0.15	0.33	0.71	0.14	1.07	1.33	0.10	0.30	0.42	0.09	1.07	0.32	0.22	0.56
Tb	0.03	0.06	0.07	0.02	0.11	0.23	0.02	0.05	0.07	0.02	0.20	0.06	0.03	0.10
Dy	0.20	0.40	0.31	0.12	0.49	1.57	0.13	0.35	0.45	0.13	1.41	0.44	0.18	0.73
Ho	0.05	0.09	0.05	0.03	0.08	0.33	0.03	0.08	0.10	0.03	0.32	0.10	0.04	0.16
Er	0.14	0.27	0.15	0.08	0.19	0.89	0.08	0.22	0.29	0.11	1.02	0.29	0.11	0.46
Tm	0.02	0.04	0.02	0.01	0.02	0.13	0.01	0.04	0.04	0.02	0.17	0.05	0.02	0.07
Yb	0.17	0.29	0.13	0.08	0.12	0.91	0.10	0.24	0.29	0.14	1.33	0.32	0.13	0.44
Lu	0.03	0.05	0.02	0.01	0.02	0.14	0.01	0.04	0.05	0.02	0.21	0.05	0.02	0.07
Hf	0.07	0.11	0.54	0.16	0.14	0.57	0.05	0.19	0.25	0.06	0.70	0.14	0.17	0.25
Ta	0.05	0.01	0.08	0.04	0.13	0.02	0.03	0.02	0.02	0.00	0.22	0.02	0.04	0.01
W	0.09	0.03	0.04	0.04	0.01	0.11	0.01	0.05	0.04	0.07	0.50	0.04	0.44	0.03
Pb	1.95	2.68	3.50	6.26	0.93	3.14	2.05	0.77	1.61	1.15	5.72	1.49	1.09	2.52
Th	0.03	0.08	0.39	0.10	0.03	0.01	0.01	0.07	0.10	0.03	1.32	0.07	0.23	0.05
U	0.01	0.03	0.16	0.06	0.01	0.01	0.01	0.03	0.04	0.01	1.02	0.03	0.12	0.03
PGE ppb														
Os	10.1	8.45	NA	NA	NA	NA	1.95	NA	NA	NA	NA	NA	NA	0.34
Ir	14.3	14.36	NA	NA	NA	NA	2.60	NA	NA	NA	NA	NA	NA	0.44
Ru	41.6	36.78	NA	NA	NA	NA	8.14	NA	NA	NA	NA	NA	NA	1.45
Rh	75.7	63.93	NA	NA	NA	NA	12.8	NA	NA	NA	NA	NA	NA	0.48
Pt	1020	1045.98	NA	NA	NA	NA	151	NA	NA	NA	NA	NA	NA	3.67
Pd	2902	2077.50	NA	NA	NA	NA	467	NA	NA	NA	NA	NA	NA	5.32
Au	158	168.53	NA	NA	NA	NA	27.7	NA	NA	NA	NA	NA	NA	1.17

Correlation	Pt	Pd	Rh	Au	Cu	Ni	S
Pt	1	0.85	0.71	0.58	0.52	0.56	0.38
Pd	0.85	1	0.72	0.62	0.62	0.66	0.47
Rh	0.71	0.72	1	0.19	0.13	0.34	0.1
Au	0.58	0.62	0.19	1	0.74	0.45	0.45
Cu	0.52	0.62	0.13	0.74	1	0.66	0.74
Ni	0.56	0.66	0.34	0.45	0.66	1	0.62
S	0.38	0.47	0.1	0.45	0.74	0.62	1

Table 2: Correlation coefficients between the various metals and PGE using the PTM assay database for the project area (9573 samples except for Rh with 2717 samples).